Crystal Growth of Calcium Carbonate in Hydrogels as a Model of Biomineralization

*Emily Asenath-Smith, Hanying Li, Ellen C. Keene, Zhi Wei Seh, and Lara A. Estroff**

In recent years, the prevalence of hydrogel-like organic matrices in biomineralization has gained attention as a route to synthesizing a diverse range of crystalline structures. Here, examples of hydrogels in biological, as well as synthetic, bio-inspired systems are discussed. Particular attention is given to understanding the physical versus chemical effects of a broad range of hydrogel matrices and their role in directing polymorph selectivity and morphological control in the calcium carbonate system. Finally, recent data regarding hydrogel-matrix incorporation into the growing crystals is discussed and a mechanism for the formation of these single-crystal composite materials is presented.

1. Introduction

Historically, the use of gel matrices for single crystal growth has been employed as a means to control the purity, morphology, and optical quality of the resulting crystals.[1,2] More recently, crystal growth in gels has emerged as a popular platform for modeling biomineralization processes.[3–9] This interest is motivated by the increasing number of gel-like matrices identified in association with mineralization by biological organisms (**Table 1**).

In matrix-mediated biomineralization, the mineralization environment is characterized by the presence of an extracellular matrix, which is a three-dimensional macromolecular assembly of proteins, polysaccharides, and/or glycoproteins that mediates mineral formation.[46,47] These matrices are often fibrous, porous, and hydrated networks that both provide the structural framework upon which inorganic minerals grow and serve as a source of chemical functionalities to direct nucleation and growth of the crystals.[48–50] Often these organic matrix constituents are intimately associated with the inorganic crystals, and are sometimes even incorporated into the single crystals, thereby forming composite materials with unique optical, mechanical, or structural properties.[51–53]

The repeated theme of biomineralization in gel-like organic matrices provides new opportunities for the classical approaches to crystal growth in gels. What was once seen as a means to obtain large crystals of high purity is now being employed as a method to both answer questions from biology as well as to create new composite materials with "designer" properties. For example, gel-based systems may help elucidate the origins of biological control over polymorph selection,[54,55] crystal orientation,[35] morphology,[21,56] and matrix incorporation.[21,57] Synthetically, crystal growth in gels can provide routes to achieve the controlled introduction of nanoscale inclusions to single crystals,[58] to access nonclassical mesocrystal structures,[59,60] and obtain diverse morphologies.[61,62]

This article highlights both the biological motivations for crystal growth in gels as well as recent innovations in the application of synthetic gel-based systems for controlling crystallization. The examples presented here showcase the insights gel-growth can provide regarding the structure and formation of biominerals, including the role of the water-insoluble matrix, the role of chemical modification of the matrix, and the mechanisms by which the organic-matrix can become incorporated into the crystals during growth. These bio-inspired, synthetic approaches hold the potential to yield whole new classes of composite materials such as polymer-reinforced single crystals and mesocrystal architectures.

2. Background

Crystal growth in gels is a modification of crystal growth in solution and has been used as a crystal growth technique for more than one century.[1,2] The unique aspects of crystal growth in gels derive from the compartmentalization of the solution into small cavities within the three-dimensional porous gel network. This solute confinement has implications for nucleation and growth mechanisms as well as the morphology of the resulting crystals. In the following sections, we introduce the chemical and structural features of several types of gels commonly used for crystal growth and provide a brief overview of classical crystal growth mechanisms. Subsequently, nucleation and growth considerations will be discussed in the context of gel systems, followed by an overview of experimental techniques for crystal growth in gels.

2.1. Common Gels Used for Crystal Growth

A gel is defined as a two-component (solid and liquid), continuous, solid-like material with viscoelastic rheological

E. Asenath-Smith, Dr. H. Y. Li,[+] Dr. E. C. Keene, Z. W. Seh, Prof. L. A. Estroff
Department of Materials Science and Engineering
Cornell University
Ithaca, NY 14853, USA
E-mail: lae37@cornell.edu
[+] Current address: Dr. H. Y. Li, Zhejiang University, Department of Polymer Science and Engineering, Hangzhou, P. R. China

DOI: 10.1002/adfm.201200300

properties.[63,64] Put more simply, a solution is considered to be a gel when it no longer flows and can support its own weight (e.g., the inverted test-tube test). From a broad perspective, gels can be classified according to the type of bonding within the network. Of the four gel types proposed by Flory,[65] only the two most relevant to biomineralization will be formally discussed: physical gels and chemical gels. In physical gels, the network is primarily formed through physical entanglement and non-covalent intermolecular forces. The network in chemical gels is formed via covalent bonds, which can be formed by reactions such as free-radical polymerization by UV light or chemical initiators. Gel networks are often classified as cellular or fibrous, or a mixture of both depending on the network characteristics (**Figure 1**).

Characterization of gel structures is inherently difficult because of the low polymer/organic content and high solvent content. Most sample preparations introduce drying artifacts, thereby producing an image that may not be a completely accurate representation of gel conditions present during crystal growth.[66–70] For example, drying techniques can cause the gel structure to collapse and freezing techniques can introduce ice crystals, which may cause structural distortion of the gel network.[71] Additionally, the recipe (in particular the solution) to prepare gel samples for structure characterization is usually different from that used for crystal growth. As discussed below, this difference often results in structural changes to the gel network. Finally, gels are not equilibrium structures and most likely there is structural evolution that occurs over timescales similar to those used for crystallization experiments.[72,73] While entire books and reviews have been written about gels and gelators,[64,74–78] here we highlight the chemistry and structure of several gels that are commonly used to study biomineralization.

2.1.1. Gels with Physical Bonding

Physical gels are the most commonly encountered class of hydrogels in biomineralization systems. They are often composed of biopolymers of polysaccharides such as agarose, pectin and cellulose, as well as proteins such as collagen, gelatin and silk fibroin.[64] The network in physical gels is formed through physical interactions, including, but not limited to, hydrogen-bonds, hydrophobic, or Coulombic forces, among biopolymer chains.[79] Secondary structural features of biopolymers can further influence the structure of the network formed in physical gels. Gelation of physical gels can be achieved by temperature, solvent or pH changes, with the potential for reversibility.[65] The physical nature of the bonding interactions in these gels can vary with temperature and time, imparting some dynamic character to the structure of these networks.

Agarose. Agarose is a neutral polysaccharide that is derived from red algae.[80] The molecular structure of agarose is a neutral, linear polysaccharide consisting of alternating 1,3-linked β-D-galactopyranose and 1,4-linked 3,6-anhydro-α-L-galactopyranose units[81] and consequently is regarded as a relatively inert medium for crystal growth. Agarose powder is soluble in hot water and the warm solution gels on cooling to ≈40 °C. Agarose gels melt at ≈85 °C, noticeably higher than the gelling temperature. During the process of gelation, polymer chains form helices (double or single helices) that subsequently aggregate into three-dimensional (3D) bundles, forming a porous network with fibrous characteristics (Figure 1a,b).[82,83] Both the gelling and melting temperatures can be tailored by chemical modification such as partial hydroxyethylation.[84] The mechanical behavior of agarose gels is sensitive to molecular weight and concentration[85] as well as chemical modification.

Lara A. Estroff is an assistant professor of Materials Science and Engineering at Cornell University. She studied chemistry throughout her education, beginning at Swarthmore College (B.A.), continuing at Yale University (Ph.D.) and Harvard University (post-doctoral researcher). She also spent time at the Weizmann Institute of Science in Israel, where she was introduced to biomineralization. Dr. Estroff's research focuses on bio-inspired materials synthesis, in particular, crystal growth in gels and its relationship to biomineralization.

Hanying Li is a professor in the Department of Polymer Science and Engineering at Zhejiang University, China. He received his Ph.D. in Materials Science and Engineering from Cornell University (advisor: Prof. Lara A. Estroff). After postdoctoral work on organic electronics at Stanford University (Prof. Zhenan Bao's group), Dr. Li moved to Zhejiang University in December 2011. His current research focuses on bio-inspired single-crystal growth and organic-single-crystal-based electronic and optoelectronic devices such as transistors and solar cells.

Emily Asenath-Smith received her B.A. in Chemistry from Mount Holyoke College and subsequently completed her M.S. in Ceramic Engineering at Alfred University. She is currently working in the research group of Prof. Lara Estroff as a Ph. D. candidate in Materials Science and Engineering at Cornell University. She is a fellow of the IGERT Program in Materials for a Sustainable Future and is researching crystal growth in gels as a means to form nanocomposites.

Table 1. Biomineralization systems with hydrogel-like organic matrices.

Biogenic system	Mineral	Gel-like matrix components	Water-soluble matrix components	References
Mollusks, nacre	Aragonite	Silk fibroin-like hydrogel	Acidic proteins	[10–12]
Coral	Aragonite	Fibrillar, non-collagenous proteins	Acidic (sulfonated) glycoproteins	[13–19]
Otoconia	Calcite	Short-chain meshwork-forming collagens (e.g., Otolin-1)	glycoproteins Otoconins	[20–24]
Otoliths	Aragonite, Vaterite, Calcite	Short-chain meshwork-forming collagens (e.g., Otolin-1)	OMP-1	[25–33]
Barnacles	Calcite	α-chitin and other unidentified protein(s)	Acidic proteins	[34]
Enamel	Carbonated apatite	Amelogenin	Glycoproteins (e.g., enamelin)	[35–38]
Bone	Carbonated apatite	Fibrillar collagen	Acidic glycoproteins Gla proteins Proteoglycans	[39–42]
Chiton/limpet teeth	Hydrous and non-hydrous iron oxides	α-chitin and other unidentified protein(s)	Not yet well-characterized	[43–45]

The pore sizes within agarose gels have been found to depend on a number of factors. First, pore sizes depend on the concentration of agarose used (Figure 1a,b). For example, when gel concentration increased from 0.5 wt% to 5 wt%, pore sizes were observed by SEM to decrease from 180 nm to 55 nm.[71,86,87] Secondly, the pore sizes within agarose networks depend on the solvent used. For example, gels prepared with aqueous Tris-borate buffer have larger pore sizes than those gels made in deionized water.[67] Further, the diameter of agarose fibers can vary from 3–30 nm depending on experimental conditions.[67,88,89]

Silk Fibroin. Silk fibroin is the structural component of silk fibers, and is composed of disulfide-linked polypeptides, which exist in anti-parallel β-sheets and are predominantly composed of the amino acids glycine, alanine, and serine.[90] In the formation of a hydrogel, silk fibroin undergoes gelation through hydrophobic and hydrogen-bonding interactions, forming a network with mixed fibrous and cellular character (Figure 1c,d). Gelation times are found to decrease with increasing silk fibroin concentration, increasing temperature, and decreasing pH.[90,91] Further, the secondary structure is found to vary from random coil to β-sheet with changes in pH and ionic concentration, thereby influencing the structure of the hydrogel network; the hydrophobic regions in random coil silk fibroin assemble in aqueous solutions via hydrophobic interactions and organize into β-sheets, physically cross-linking the hydrogels.[92] Pore sizes in silk fibroin hydrogels decrease with increasing silk fibroin concentration as well as temperature, showing ≈1 μm pore sizes in a freeze-dried 4 wt% silk fibroin hydrogel.[90] Gelation rates and the mechanical properties of the resulting gels are also strongly dependent on the purification method used to obtain the silk fibroin (Figure 1c,d).[93]

Gelatin. Gelatin is derived from the partial hydrolysis of collagen, which contains ≈30% glycine, ≈15% of each proline and hydroxyproline, ≈4% lysine and ≈8% arginine, and aspartic and glutamic acids each present at 7-10%.[77,94,95] More simply put, gelatin contains both acidic and basic amino acids, causing the isoelectric point of gelatin to depend on the preparation/extraction conditions. Acid-based protocols result in gelatins (Type A) with isoelectric points in the basic range (pH≈ 9), while alkaline-based protocols result in gelatins (Type B) with acidic isoelectric points (pH ≈5).[77] Similar to other physical hydrogel systems, gelation in gelatin proceeds thermally, occurring at ≈30 °C. In addition, gelatin can be chemically crosslinked through carboxylic acid groups, to increase thermal stability and change the mechanical properties of the gel.[76,96] Gelatin forms cellular networks, with cavities on the order of tens of micrometers, which are defined by non-porous walls.[72]

2.1.2. Gels with Chemically Bonded Networks

Chemical gels, also appropriately referred to as polymer or synthetic gels, are generally non-biological in origin. In this category of gels, the 3D network structure is formed through covalent crosslinks between structural units of the polymer chains. These reactions proceed by UV-initiated copolymerization in the case of polyacrylamide and acid- or base-catalyzed condensation in the case of silica. Generally, gelation is not reversible in chemical gels.

Polyacrylamide. Formation of polyacrylamide (PAA) proceeds by radical copolymerization of acrylamide and *N,N'*-methylenebis(acrylamide), forming a covalently crosslinked hydrogel with potentially variable crosslink densities. Gelation times are affected by the crosslink density,[97] as are the cellular

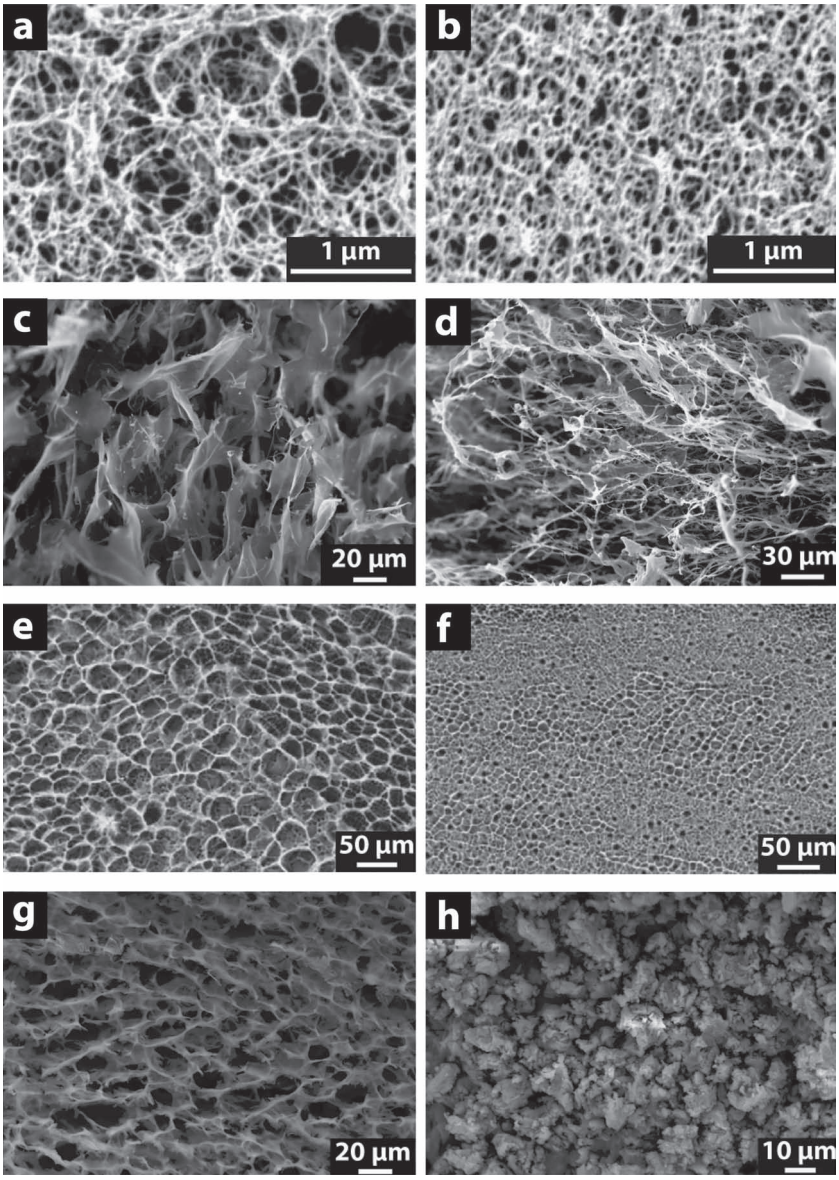

Figure 1. Hydrogel microstructures imaged by scanning electron microscopy (SEM) that illustrate the wide range of microstructures available in hydrogels as well as the factors that further influence those microstructures. Critical point dried agarose gels showing the dependence of microstructure on concentration: a) 0.5 wt% and b) 2 wt%. Freeze-dried silk fibroin hydrogels showing the dependence of microstructure on purification method: c) purified with Marseilles soap and d) purified with sodium carbonate. Freeze-dried polyacrylamide hydrogel microstructure showing the effect of gel concentration on the microstructure: e) 5 wt% and f) 10 wt% polyacrylamide gel. Freeze-dried silica hydrogels showing the dependence of microstructure on pH: g) pH ≈ 9 cellular microstructure and h) pH ≈ 2 particulate microstructure. Panels (a,b) adapted with permission.[86] Copyright 2006, American Chemical Society. Panels (e,f) adapted with permission.[99] Copyright 2008, Elsevier.

characteristics of the network.[66,98] The wall thicknesses of the cellular network in PAA hydrogels are found to increase with increasing PAA concentration in the gelling solution.[70] Pore sizes within the cellular network depend on the concentration of the gelating compound, showing a decrease from 150 nm to 30 nm with an increase in polymer concentration from 5 wt% to 10 wt% (Figure 1e,f).[99] Further, the pore size distribution can be broad, causing a range in the polymer density within the gel medium.[100]

Silica gels. Silica gels are traditionally the most widely used gels for crystal growth. While silica gels can be formed from the acidification of both alkoxyorthosilicates and sodium metasilicate, the latter will be emphasized in the following discussion. Silica hydrogel formation in sodium metasilicate systems proceeds by three distinct steps: i) dissolution of Na_2SiO_3 in water to form silicic acid ($Si(OH)_4$) and sodium hydroxide: $Na_2SiO_3 + 3H_2O \Leftrightarrow 2NaOH + Si(OH)_4$; ii) acid-catalyzed polymerization of silicic acid by condensation to form 3D clusters; and iii) percolation to form a 3D gel network. Through these processes, the network structure in silica hydrogels is established predominantly through covalent interactions[2,64] to form a basic hydrogel composed of cellular networks with porous walls (Figure 1g). The thickness and porosity of the cell walls depends on the concentration (density) of silicate species used in the gel.[72] The gelation time varies with silicate reactant concentration,[101] pH,[102] temperature,[103] and the identity of the acid catalyst[104] and affects the final structure of the hydrogel network. For example, acidification with stronger acid results in longer gelation times, forming acidic gels that are composed of networks with particulate character (Figure 1h).

2.1.3. Mixed Bonding Character and Solvent Structure in Gel Networks

The broad categories of physical and chemical hydrogels discussed above do not always strictly apply. For example, gelatin networks can contain a combination of physical and chemical crosslinks depending on preparation conditions. Further, linking between silica clusters during percolation may be physical and/or covalent in nature, thereby imparting some physical characteristics to the structure.[105,106] Moreover, since gelation is a dynamic event, the network structure can continue to evolve even after the onset of the generally accepted "gel point": when the gel resists pouring. For example, physical gels evolve with temperature and time as discussed above, and condensation in chemical gels, such as silica, is also temperature and time dependent.[2] As such, all of these factors require attention when preparing and characterizing hydrogels.

Lastly, for crystal growth in gels, it is important to consider the structure of solvent molecules, as they behave differently than their bulk counterparts when confined to the pores of a hydrogel network. In gels, liquids are trapped within regions

defined by the solid network. The interaction at the solid/liquid interface changes the structure of liquids nearby the interfaces.[107,108] For example, water in hydrogels has been studied[109–114] and found to exhibit three distinct structures: bound water, free water, and intermediate water.[115–117] The bound water interacts strongly with the solid network and has aggregation structures that are different from the bulk water. Free water behaves most similarly to bulk water. The intermediate water interacts weakly with the solid network and is in a state that is not bound or free, but structured.[70] Of importance for crystallization studies in gels, these differences in solvent structure will lead to changes in the activities of solutes thereby affecting both the relative supersaturation and the diffusion rates of solutes within the gel media.

2.2. Crystal Morphology and Crystal Growth Mechanisms

Before discussing crystal growth in hydrogel media, it is important to review, briefly, classical crystal growth mechanisms and their role in defining crystal morphology. Over a century of study on crystal growth has identified several critical relationships among the thermodynamic and kinetic constraints on growth dynamics and the corresponding morphologies of the crystals.[118–120] In crystal growth from solution, as opposed to growth from a melt, the basic thermodynamic driving force is manifest in the supersaturation.[118] The supersaturation (σ) is directly related to the solubility product (K_{sp}) and the activity product (AP) of the ionic species according to $\sigma = \ln\left(AP / K_{s\rho}\right)$.

As a function of the driving force and the crystallization kinetics, several key crystal growth regimes have been identified.[48,121,122] Near-equilibrium growth occurs at low supersaturation via addition to step edges formed by screw dislocations (spiral growth). Crystals formed in this regime have well-defined facets and smooth surface features, displaying equilibrium polyhedral morphologies. At slightly higher driving forces (supersaturation), layer-by-layer growth occurs via addition to step edges formed by the nucleation of 2D islands. Hopper or skeletal morphologies can be observed in this regime and are characterized by concavities on the faces resulting from the increased rate of nucleation at the corners of the growing crystal. As the supersaturation is increased further, growth proceeds by the nucleation of 3D units on the surface, leading to fractal, dendritic morphologies. Finally, at the highest supersaturation, the critical nuclei radius can be smaller than a unit cell and continuous adhesive growth occurs, leading to aggregated spherulitic morphologies with rough surfaces. Accordingly, crystal morphology can be used as an initial guide to unraveling the probable growth mechanisms that led to the final morphologies observed for crystals grown in different gels and under different conditions.

2.3. Crystal Nucleation and Growth in Gels

Crystal growth in gels has been widely used to prepare single crystals of proteins for structural characterization,[123–129] to synthesize porous materials,[86] and to simulate crystallization in microgravity conditions.[127] Much of the early work on crystal growth in gels has been reviewed and collected by Henisch[2] and Lefaucheux and Robert.[1] Herein, we focus on the development of crystal growth in gels as a model for biomineralization systems.

Similar to the organic matrices found in biomineralization systems, the local crystallization microenvironment in gel media is distinguished from that in solution by the confinement of solutes to within the pores of the gel network. Empirically, this microenvironment presents several advantages in crystal growth studies: Brownian motion, laminar flow, and convective currents are suppressed, making diffusion the dominant mass transport mechanism available to solutes in gel media. Further, gel networks are capable of supporting the growing crystals, preventing sedimentation. Overall, these conditions present a means to obtain large, high quality crystals.

2.3.1. Nucleation

Detecting nucleation events within a gel is inherently difficult and complicates a quantification of the absolute supersaturation level present at nucleation. In addition, time-dependent gradients are formed within the gel as reactants diffuse through the gel to the reaction front.[130] These additional experimental complexities are not addressed by classical nucleation theory.[131,132] Thus for nucleation in gels a threshold supersaturation is defined, which represents the supersaturation level present when nucleation can be visually observed in the gel.[133] Generally, within a diffusion-limited medium, there is a reduced probability that nuclei reach the critical size required for growth due to the diffusion-limited supply of reactants. Therefore, nucleation in gels takes place only when solutes accumulate to a fairly high threshold supersaturation.[133,134] As a result, gels can be used to control the rate of nucleation to yield a smaller number of crystals with larger sizes than their solution-grown counterparts.[135]

To further complicate matters, the gel itself can affect the supersaturation threshold due to chemical functionality within the gel network, which can interact with solutes to suppress or enhance nucleation. If the gel fibers or "walls" themselves can act as heterogeneous nuclei, then the original picture changes and higher nucleation densities will be observed within the gels than in solution. For example, lead iodide and calcium tartrate have increased nucleation densities in gelatin, as compared to silica gels.[72] Other studies have demonstrated that nucleation rates of hen egg white lysozyme depend strongly on the type of gel used (e.g., silica versus agarose).[105,136,137] Further emphasizing the role of the gel, nucleation rates of other proteins in agarose gels have been found to depend on the agarose concentration.[138] Thus, the supersaturation threshold for a given species depends on more than just the type of gel in which the nucleation is taking place.

2.3.2. Growth

The diffusion-limited conditions present in gels cause a modification to the crystal growth regimes and resulting morphologies discussed in Section 2.2. Whereas the morphology of solution-grown crystals is dictated by the driving force (σ) alone, the morphology of gel-grown crystals represents a balance between

the driving force and the diffusion rate(s) of ions to the reaction front.[61,139] Due to this diffusive transport, concentration (and corresponding supersaturation) gradients are formed at the interface, introducing the potential for corners and edges of growing polyhedral crystals to experience higher supersaturation, and thus faster growth rates. This kinetic and thermodynamic balance is seen in crystals grown in gels under supersaturation conditions that favor 2D growth mechanisms: hopper morphologies result from faster delivery of solutes to corners as opposed to faces.[2,140] Other experimental parameters such as temperature influence crystal growth in gels through the temperature dependence of diffusion coefficients and crystal solubilities. In general, diffusion coefficients increase by 2–3% per °C from a given value at 25 °C,[141] whereas the solubilities, and thus the supersaturation levels, may increase or decrease with temperature, depending on the system. Further, gel density can be an effective means to control growth rates in gel media, where increased gel concentration results in smaller pores and thus higher apparent supersaturation, increasing growth rates and affecting the observed morphologies.[61]

In addition to "generic" effects of gels on growth, specific (chemical) interactions between crystal-gel pairs have been suggested by many studies. For example, growth in agarose gels has been used to control the enantiomeric selectivity of sodium chlorate,[142] and the crystal morphology of multiple inorganic salts has also been shown to vary strongly as a function of gel type.[4,143–146] Finally, incorporation of the gel media into the growing crystals is known,[58,123,147–149] and may depend on both chemical and physical factors, as described further in Section 4.3. These studies and others demonstrate the wide range of crystal growth conditions that can be achieved in gel media and highlight that there is still much to be learned about crystal growth mechanisms in gels.

2.4. Crystallization Techniques for Growth in Gels

Before describing the use of gels to model biomineralization, it is important to discuss some of the practical aspects of crystal growth in gels. As in solution crystallization, the key for gel growth is to trigger nucleation and then allow for slow, controlled growth of the crystal(s). For precipitation reactions involving two components (A and B), there are two typical methods for introducing A and B to the gel: single and double diffusion geometries (**Figure 2**). In a single diffusion set-up, one component is embedded in the gel and the other one is introduced either via a solution layered on top of the gel (Figure 2a) or as a gas phase above the gel (Figure 2b). In this geometry, the crystals are usually found near the solution/gel or vapor/gel interface. Often a dense band of precipitate will be located at this interface, with larger, single crystals further down the gel column. When double diffusion is used, reservoirs containing solutions of the two reagents are physically separated on two sides of a gel column, in a U-tube or straight-tube configuration (Figure 2c), allowing diffusion of the two components into the gel from opposite ends. During the experiment, gradients of pH and concentration (supersaturation) that change with time develop along the length of the gel column, allowing access to a spectrum of conditions in one experimental set up. Generally,

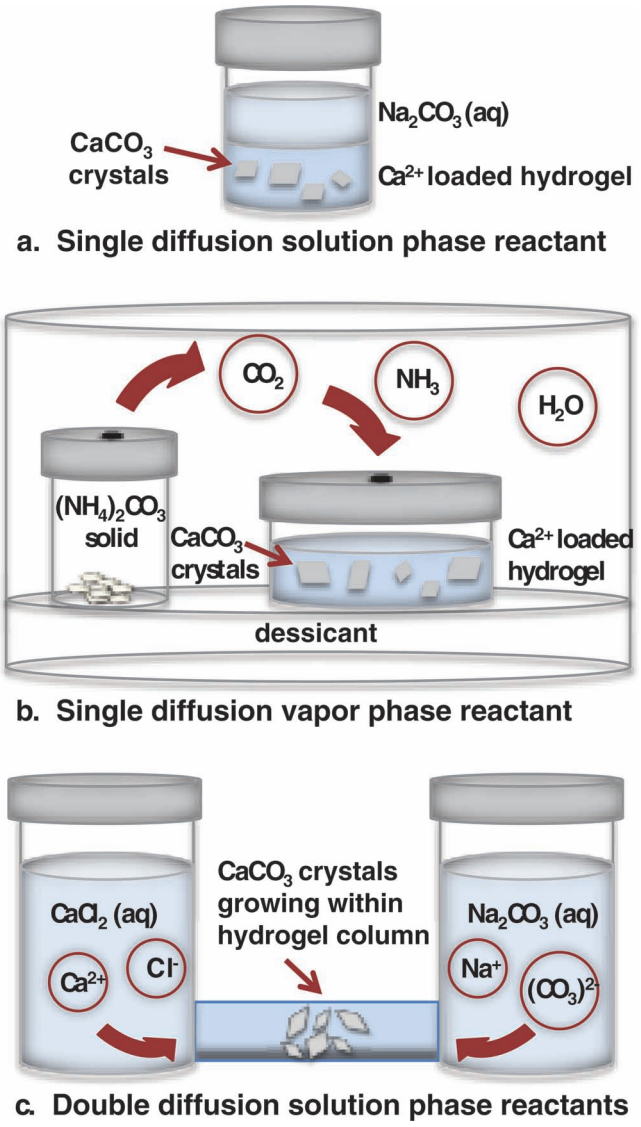

Figure 2. Schematic representation of experimental approaches used to grow calcium carbonate crystals in hydrogels: a) in the solution-based single diffusion set-up, the solution phase reactant diffuses into the gel; b) in the vapor phase single diffusion set-up, the vapor phase reactant diffuses within the sealed atmosphere of a dessicator, and reaches the hydrogel through a small hole in the lid; and c) in the solution-based double diffusion system, aqueous solutions of the two reactants diffuse into opposite ends the gel and meet in the middle.

a band of crystals is observed to form near the center of the gel, but the exact location of crystallization depends on the gradients created along the length of the gel. Both single and double diffusion methods can be used to grow poorly soluble crystals, such as those of interest in modeling biomineralization, from two (or more) soluble reagents.[2,150] For all of these systems, it is essential to understand the underlying diffusion laws in order to predict when and where crystal growth will occur and how supersaturation gradients will evolve over the course of the reaction.[151,152]

For single-component crystals (e.g., proteins and small organics), or highly soluble salts, additional strategies are

required to trigger nucleation. For example, the single-diffusion geometry can be used to introduce a precipitant, such as a non-solvent, either via solution or vapor phase.[149,153] Alternatively, crystallization can be induced by a change in a physical parameter, such as temperature.[144]

3. Biogenic Calcium Carbonate Systems that Mineralize in Gel-Like Media

Calcium carbonate, which exists as one of three polymorphs (calcite, aragonite, and vaterite), as well as amorphous forms, is the most common biomineral found in nature.[40] The matrix associated with calcium carbonate biominerals is often described as having water-soluble and water-insoluble fractions. The water-insoluble components form the structural framework of the crystal growth environment, while the water-soluble components impart chemical functionality, thereby affecting nucleation and growth.[48] The water-soluble components are predominantly acidic biomacromolecules, which may include carboxylated, sulfonated, and/or phosphorylated glycoproteins and proteoglycans.[50,154,155] In the last 10 years, some of the protein- and polysaccharide-based components of the water-insoluble matrices have been identified as having a hydrogel-like character (Table 1). Here, we discuss several representative calcium carbonate systems that mineralize in gel-like matrices, however, mineralization in gel-like media has also been described for calcium phosphate systems. For example, enamel develops in a gel-like matrix of amelogenins,[35] and bone and dentin form in a fibrous, collagen-based matrix.[39]

3.1. Nacre (Mother-of-Pearl)

Nacre, the inner layer of some mollusk shells, is a composite structure with ≈500 nm thick single-crystal aragonite lamellae interspersed with ≈30 nm thick layers of organic matrix.[11] The organic matrix amounts to 2–5 wt% of the dry shell. The aragonite tablets grow within a pre-formed organic matrix (**Figure 3**a) that is composed of water-soluble acidic proteins[155] and water-insoluble β-chitin fibers and a silk fibroin-like hydrogel.[10,11,156] Each of these matrix components has a role in controlling the crystal polymorph and orientation (nucleation), as well as morphology (growth), though none are thought to function in isolation and their assembly and interaction may be essential for correct regulation of crystal growth in vivo.[11,157,158] The crystallographic orientation of the aragonite platelets is related to the orientation of the β-chitin fibers and thus β-chitin is assigned a role in directing crystal orientation, while the acidic proteins decorate the chitin surface forming nucleation sites.[11] The silk fibroin hydrogel contains additional acidic proteins, which are believed to control crystal polymorph and/or morphology. During mineral formation, acidic proteins are trapped within the aragonite crystals, while the hydrophobic hydrogel is pushed aside to regions between adjacent crystallites.[11]

In the organic matrix of *Atrina rigida*, a silk fibroin-like protein has been found to make up the largest weight fraction of the total protein content.[11] Based upon cryo-TEM and environmental SEM (ESEM) imaging of nacre, a gel-like phase has been identified.[10,11,54] In the ESEM images, as the pressure is reduced, a protein-based substance is seen "oozing" from between the aragonite tablets (Figure 3b). This proteinaceous gel-like material is hypothesized to be the silk-fibroin-like protein. Lending support to this hypothesis, silk fibroin proteins are known to form hydrogels in vitro (Figure 1c,d).[90,91,93] As a predominately hydrophobic constituent,[95] the silk fibroin-like gel in nacre has been suggested to inhibit calcite crystallization, thereby favoring growth of the less stable polymorph aragonite.[11] The gel could also serve as a "space-filler" that pre-fills the cavity into which the aragonite tablets grow. In this model, as the crystals grow, the gel itself is compressed and excluded to the crystal-crystal interfaces.[54]

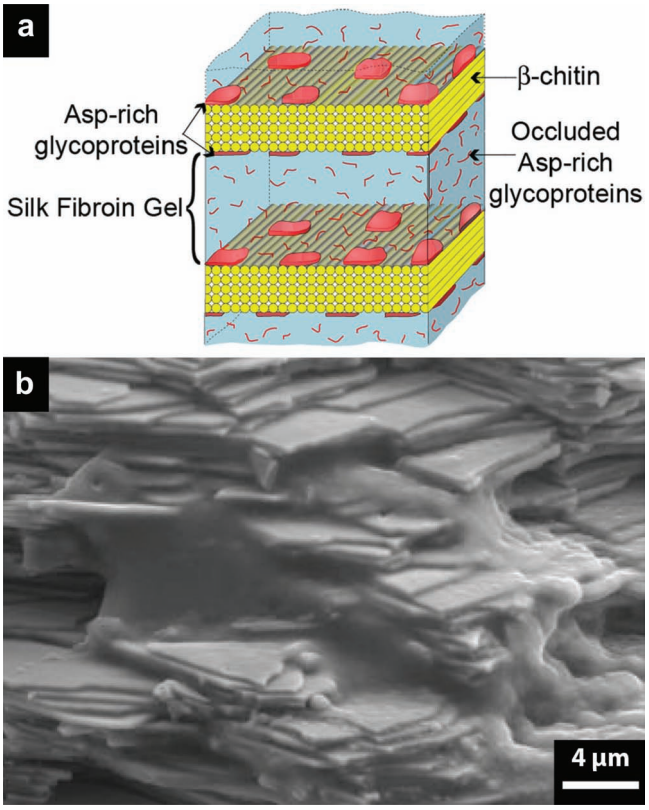

Figure 3. a) Schematic of the demineralized organic matrix of *Atrina rigida*, a model matrix-mediated biomineralization system. For further detail on the individual components see text. b) Environmental SEM image of nacre from *Atrina rigida* illustrating the gel-like organic matrix exuded from between aragonite tablets during drying. Panel (a) adapted with permission.[10] Copyright 2001, Elsevier. Panel (b) adapted with permission.[11]

Nacre serves as a classic biomineralization model, due to the demonstrated control over polymorph selectivity, crystal orientation, and mechanical properties. Further, the extensive chemical and structural characterization that has been reported in these systems has elucidated the role of matrix components in establishing the strict biological control seen during nacre formation. Many of the earliest in vitro studies on biomineralization were derived from nacre systems and it continues to serve as a model for in vitro studies, some of which are discussed in Section 4.1.

3.2. Coral

Both soft (octocorallia) and stony (scleractinia) corals have been found to mineralize in association with organic matrices.[159] From a structural perspective, coral architectures are composed of aragonite crystals embedded in an organic matrix, and additionally contain occluded organic material within the crystallites. While the aragonite crystallites are composed of nanocrystalline grains <100 nm, ordered aggregates >200 nm are found that appear as single crystals in diffraction studies[160] due to *c*-axis alignment of the constituent crystallites.[161] Similar to other biomineralization systems, the organic matrices associated with corals can be divided into water-soluble and water-insoluble components. The soluble portion contains as much as 30–50 mol% acidic proteins with a large fraction of sulfonated glycoproteins.[14–16] The insoluble components form a fibrous, porous network that is (in scleractinian, *Galaxea fascicularis*) composed of 26 nm fibrils.[13] In some species, the insoluble matrix components have collagenous character.[162] The characterization of these matrices as gel-like arises from observations of a fibrillar porous network associated with calcium in the scleractinian coral, *Galaxea fascicularis,*[13] as well as a visibly gelatinous mass that retains the shape of the soft coral *Isidella sp*. (bamboo coral) after decalcification (**Figure 4**a) and is seen to have a fibrillar porous network by TEM (Figure 4b).[159]

3.3. Otoconia

Crystals of calcium carbonate, located in the inner ear, form an integral component of the vestibular system of animals. In birds and mammals the calcite polymorph is found, while primarily aragonitic otoconia are found in amphibians and reptiles.[27,31,163] Across species, the glycoproteins associated with calcite otoconia are similar to each other but different than those glycoproteins isolated from aragonite otoconia.[22] Calcitic otoconia are barrel-shaped with faceted tips, as seen in the central graphic in **Figure 5** and are up to 30 μm long in humans.[20,164,165] When these single-crystals are etched, the interior is seen to contain a dense network of fibers, suggesting occlusions of the organic matrix during crystal growth. Further, these small crystals are associated with distinct fibrous, organic networks (Figure 5a–d), wherein multiple otoconia are anchored to an organic matrix, known as the otoconial membrane, forming a viscoelastic mass that can transmit displacements resulting from linear acceleration.[20,21] The soluble matrix components are glycoproteins, known as otoconins, which comprise >90% of the total soluble organic content.[22] The characterization of the insoluble matrix components as gel-like stems from the fibrous, porous network structures (Figure 5a–d) as well as their viscoelastic properties. These insoluble components are found to be short chain, meshwork-forming collagens, known as otolins, which also comprise the insoluble components of otolith matrices (Section 3.4).[166]

3.4. Otoliths

Similar to the otoconia discussed in Section 3.3, teleost fish detect linear acceleration and gravity as well as receive sound signals through polycrystalline aggregates of calcium carbonate, known as otoliths (**Figure 6**a). While multiple otoconia are assembled in a collective mass, only three single otolith pairs occur in fish, each in a separate region of the inner ear. Otoliths are composed of aragonite and vaterite polymorphs, each with different associated (soluble) acidic macromolecules.[26] In contrast to the fibrillar collagen found in bone (and associated with nanocrystals of hydroxyapatite), the insoluble components of the otolithic membrane include a short-chain meshwork-forming collagen, known as otolin-1.[25,30,167] Similar to otoconia, otoliths are anchored to this insoluble organic membrane, which has a gel-like layer that is present both during otolithic nuclei formation and within mature otoliths (Figure 6b).[30] Otolith growth proceeds by alternating deposition of mineral and matrix,[32]

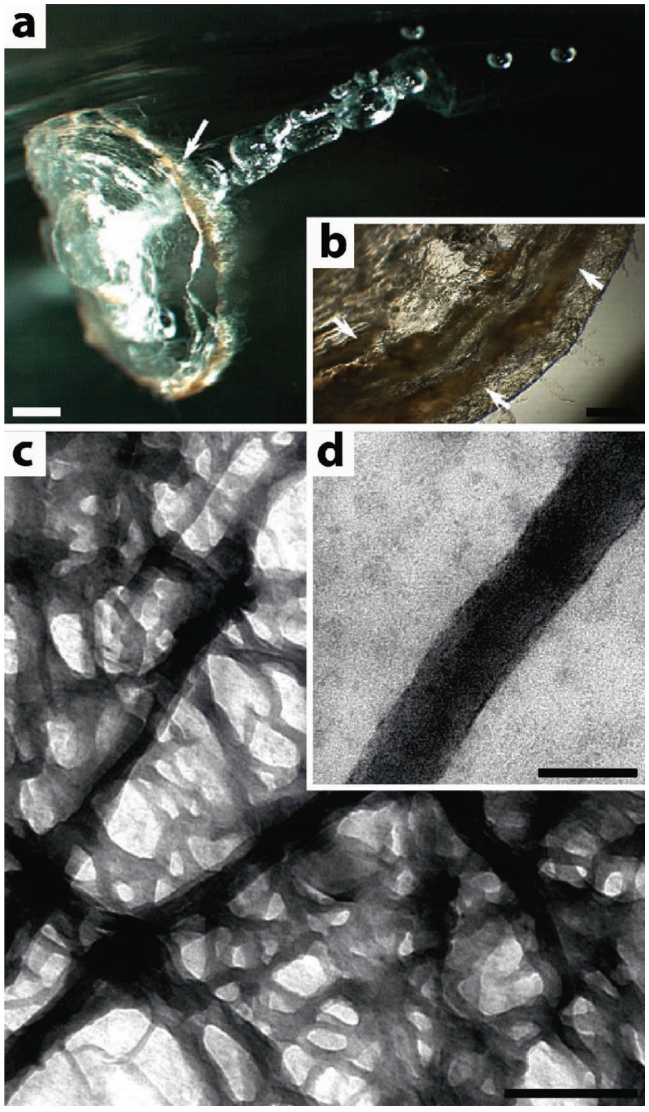

Figure 4. The non-collagenous, fibrillar, porous gel-like network associated with soft coral. Optical images of a) demineralized matrix of *Isidella sp*. and b) remaining gorgonin. c,d) TEM images showing the fibrous network of the demineralized matrix show in (a). Adapted with permission.[159] Copyright 2009, Elsevier.

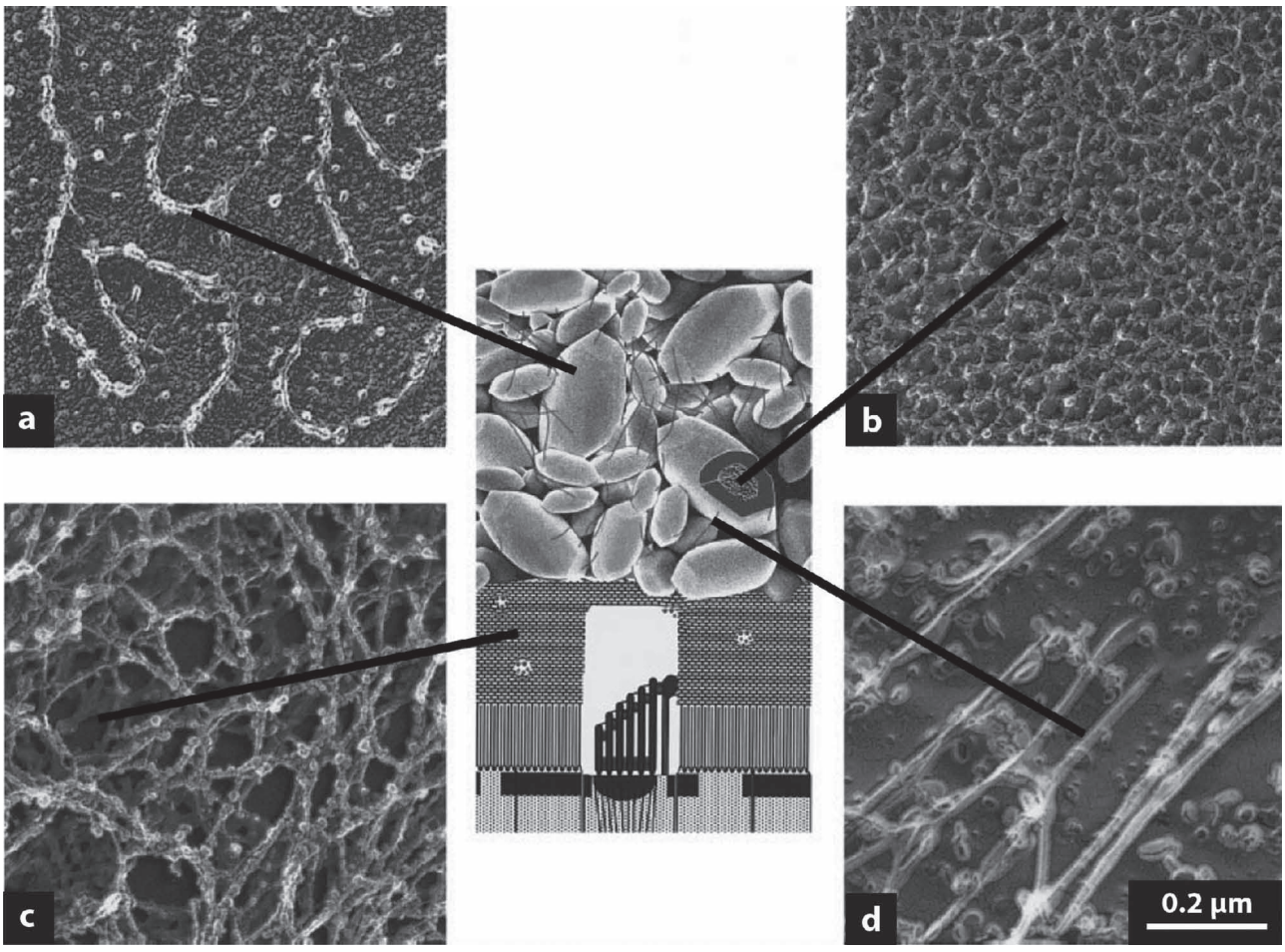

Figure 5. Different gel-like domains associated with calcite otoconia imaged by SEM with a schematic graphic showing the regional locations of each within the guinea pig vestibular system: a) filaments adhered to the surface of octoconia (≈20 nm diameter); b) the inner core of otoconia contain an organic network; c) supporting network (22 nm diameter filaments cross-linked by 11 nm filaments); and d) interotoconial matrix filaments. Adapted with permission.[21] Copyright 2000, Elsevier.

forming a organic-inorganic composite with a banded cross-section. The insoluble matrix components of otoliths have been found to retain the shape of the original crystal after decalcification with EDTA, illustrating the hydrogel-like qualities of the incorporated collagenous matrix.[25,30]

4. In Vitro Studies of Biomineralization: Crystal Growth in Gels

As discussed in the previous section, hydrogel-like matrices are associated with a diversity of biogenic systems and appear to play a role in controlling polymorph selectivity, influencing the final crystal morphology, and contributing to the materials properties of the biomineral composites. Armed with an understanding of the natural systems, hydrogel-based, bio-inspired systems have been designed to study biomineralization in vitro (Section 4.1) and to synthesize new materials.[3,145,168–170] These studies attempt to answer questions regarding the fundamental mechanism(s) that dictates polymorph selectivity, crystal orientation, organic–inorganic composite formation, and architectural assembly of complex structures. In particular, there has been a focus on the role of hydrogel matrices in defining the local crystal growth environment, both as a structural framework and as a source of chemical functionalities (Section 4.2). Finally, the factors that determine the incorporation or exclusion of the gel-like matrix into growing crystals must be clarified to enable successful composite formation in a wide variety of systems (Section 4.3). As we did in Section 3, we confine our discussion here to studies of calcium carbonate growth in gels (**Table 2**). Gel-based assays have also seen widespread use for growing calcium phosphate minerals and modeling biomineralization in bone and teeth. This work is reviewed elsewhere.[8,152,171,172]

4.1. Protein-Based Hydrogel Models for Nacre Formation

Protein-based hydrogels serve as a logical starting point when designing in vitro models of nacre due to the identification of a silk-like hydrogel in the water-insoluble organic matrix of this biomineral (Section 3.1). The first in vitro models of nacre that demonstrated polymorph control were constructed using

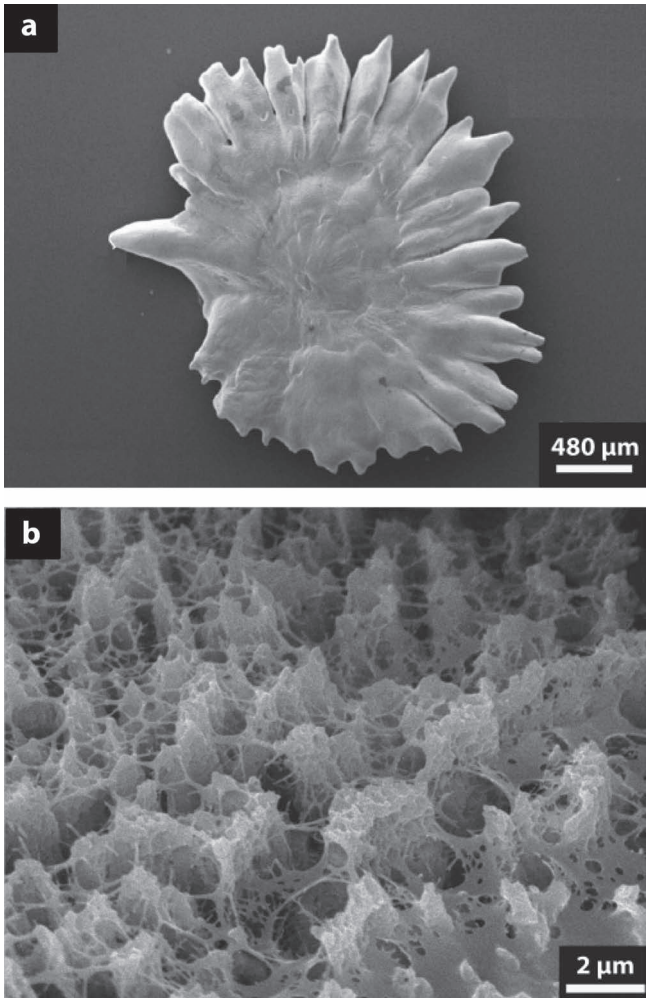

Figure 6. a) Asteriscus otolith from *Chondrostoma nasus nasus* and b) occluded matrix after de-calcification, showing a fibrous, porous organic network. Adapted with permission.[26]

water-soluble organic matrix components that were extracted from biogenic nacre, in combination with insoluble matrix components derived from other sources.[55,154,215–217] More recent in vitro models have sought to incorporate the three distinct features found in the nacre system: a fibrous substrate (e.g., β-chitin) for structural orientation; acidic macromolecules that are capable of serving as nucleation sites and controlling growth; and a hydrogel media (e.g., silk fibroin) to define the crystallization microenvironment.

4.1.1. Silk Fibroin Hydrogels

Silk fibroin hydrogels, as an analog to the silk-like proteins found in nacre, have been used to build in vitro models of nacre, due to the growing consensus that the aragonite tablets in nacre grow into a hydrated, gel-like phase.[54] Most assays to date, however, use a silk-fibroin solution or film,[216,218–223] rather than a hydrogel. Recently, we have reported a study in which silk fibroin hydrogels were coupled with β-chitin substrates and acidic peptides.[169] In previous work, we had demonstrated that when n16N, a nacre-specific peptide, is bound to a β-chitin substrate, aggregates of needle-like aragonite crystals selectively form.[212] To further increase the complexity of this matrix, we added a silk fibroin hydrogel to the peptide-chitin construct. In contrast to the results in the absence of the gel, only flattened spherulites of vaterite and amorphous calcium carbonate were obtained when all three components were present (**Figure 7**).[169] These results suggest possible changes in the binding of n16N to β-chitin caused by the addition of silk fibroin hydrogel to the matrix. The morphological changes induced by the silk gel, as well as the stabilization of the amorphous phase, however, do suggest that perhaps there is a missing component in the model that could trigger the transformation to aragonite. Importantly, changing from solution-growth to gel-growth conditions profoundly changed the crystallization results. As the field moves forward, we anticipate the role of a hydrogel matrix to become increasingly important in the design of synthetic, nacre-like architectures.

4.1.2. Gelatin Xerogels

Cross-linked gelatin xerogels with incorporated acidic polypeptides have also been used as matrices for growing calcium carbonate. When uniaxially deformed, the collagen segments become aligned, providing an analogy to the oriented β-chitin fibrils in nacre. While this model initially presents as a substrate rather than a bulk hydrogel, upon deformation and exposure to the crystallization solution, crystals grow both on the surface of the film, as well as within the swelled xerogel matrix.[168] To add acidic functionality to the gelatin xerogels, Falini and co-workers incorporated polyelectrolytes such as poly(aspartic acid) and poly(glutamic acid). They also examined the effect of inorganic additives, in particular magnesium, a known promoter of aragonite.[168,198] Dependent on the deformation state and polymer content, they observed all three calcium carbonate polymorphs, calcite, vaterite, and aragonite, with variations in crystal morphology and crystal orientation with respect to the matrix (**Figure 8**).[6,168,194–196] For example, oriented calcite crystals grew on the surfaces of the uniaxially deformed xerogels, while in the interior of the swelled films, aragonite rods grew that were oriented in the direction of the deformation.[168] The formation of the aragonite polymorph was correlated to poly-Asp content and showed no dependence on magnesium concentration.[168] At higher poly-Asp content, a switch from aragonite to vaterite is observed, suggesting that the high concentrations of anionic polypeptides leads to high local supersaturations, which in turn trigger precipitation of the kinetic polymorph.[6,194] These results support the idea that calcium carbonate polymorph and crystal morphology are largely dictated by local structural and chemical characteristics of the crystallization environment.

4.2. Hydrogels as Crystallization Matrices

As crystallization matrices, hydrogels can be used to expand both the kinetic and thermodynamic landscapes that are available to solution-based crystallization experiments. In addition

Table 2. Hydrogels and additives used in calcium carbonate crystallization.

Gel	Additives	References
Agarose	none	[3,62,149,173–177]
	cationic additives (e.g., Co^{2+}, Fe^{2+}, Ni^{2+}, Zn^{2+}, Cu^{2+}, etc.)	[178,179]
	carboxylic acids, polysaccharides	[180–183]
Charged polysaccharides (carrageenan, alginate, pectin, chitosan)	none	[62,184–192]
	cationic additives	[193]
	polyelectrolytes (e.g., poly (acrylic acid))	[190,193]
Gelatin	none	[4,145,164]
	polyelectrolytes (e.g., poly-aspartic acid)	[6,168,194–196]
	cationic additives (e.g., Mg^{2+})	[197,198]
Polyacrylamide	none	[19,60,99,145]
	polyelectrolytes (e.g., poly-L-aspartate)	[145]
	covalently functionalized (e.g., carboxylic acid)	[5,199]
Silica	none	[59,147,174,200–209]
	cationic additives (e.g., Mg^{2+}, Cr^{6+}, Mn^{2+}, Co^{2+})	[200,202,203,210,211]
Silk	none	[169]
	peptides (e.g., n16N)	[212]
Synthetic hydrogels	none	[146,213,214]

to resembling the matrix environments in which biominerals are formed, hydrogel matrices have been used to model geologic crystallization in soils and sediments.[200,203] Regardless of perspective, the answers sought by crystallization studies in hydrogels are widely aimed at distinguishing the chemical versus physical factors that determine the range of crystalline structures formed in these environments. Physically, the gel networks determine the diffusion rates of solutes, thus their local concentrations, and ultimately, the local supersaturation. In addition, gel networks have the potential to mechanically confine crystal growth (see Section 4.3). The chemistry within a hydrogel can be modulated either via the incorporation of soluble ionic species (e.g., cations) or by covalently attaching charged and/or polar functional groups (e.g., carboxylates, amines) to the hydrogel network. The presence of additional chemical functionality can influence crystallization in terms of the local supersaturation and/or by directly interacting with the growing crystal steps and facets. Carefully designed studies may be able to disentangle these chemical and physical effects and thus enable the design of synthetic crystal growth systems in gels that lead to the formation of complex crystalline structures for a wide variety of applications.

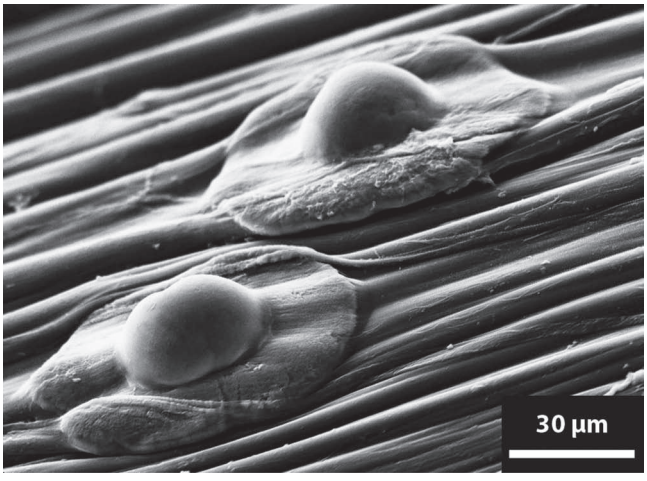

Figure 7. SEM image of calcium carbonate crystallization on β-chitin with 2.5 wt% silk fibrion hydrogel and 10 µM n16N, a nacre specific peptide. Analysis of the aggregates suggest they are a mixture of vaterite and amorphous calcium carbonate. Adapted with permission.[169] Copyright 2010, American Chemical Society.

4.2.1. Effect of Hydrogel Structure and Cationic Additives on Calcium Carbonate Crystallization in Hydrogels

In silica and agarose gels, the crystallization microenvironment is defined almost entirely by the porous structure of the hydrogel network (Section 2.1), due to the absence of strongly interacting chemical functionality within the matrix (e.g., charged groups). Thus, crystallization in these gels can be used to isolate the structural (physical) effects of the hydrogel matrix on calcium carbonate crystal growth without interference from strongly interacting chemical functionality. For example, the effects of variable pore sizes on supersaturation and crystal morphology can be examined without interference from changes in the local density of charged functional groups in the matrix. Other physical effects, such as pH, temperature and time, can also be studied. Once the physical effects of these relatively inert gel matrices are elucidated, chemical functionality can be added back into the gels in a controlled manner, such as by the introduction of soluble ions or small molecules to distinguish the physical effects of crystallization in gels from the chemical.

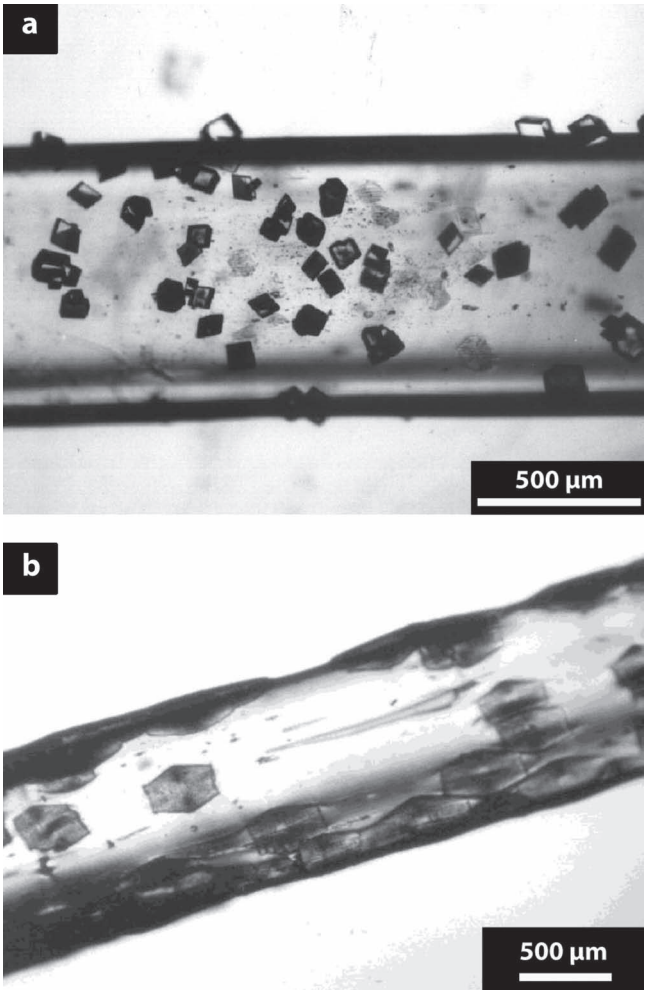

Figure 8. Optical images of calcium carbonate crystallization in uniaxially deformed (200%, elongation) gelatin films: a) Rhombohedral calcite crystals formed on film without entrapped poly(Asp). b) Aragonite aggregates formed inside the film with entrapped poly(Asp). Adapted with permission.[168]

Physical effects on morphology and polymorph. Historically, silica hydrogels have been used to grow large crystals of poorly soluble compounds using both single and double diffusion experimental configurations (Section 2.4).[2] As a growth system for calcium carbonate, double diffusion experiments allow access to a broad set of experimental conditions. The calcium and carbonate concentration gradients that form in these systems set up a continuous range of relative concentrations (and the corresponding supersaturation levels) along the gel column, allowing one to probe a number of experimental scenarios simultaneously.

Formation of the calcite polymorph in silica gels is possible over a wide range of pH and ion concentrations (supersaturations), with a diverse set of possible morphologies. At intermediate pH and low concentrations, single crystal equilibrium rhombohedra form.[200] Increasing pH or concentration can be used to shift the morphology towards hopper-like structures.[200] At high pH, polycrystalline aggregates form, including a distinct "sheaf-of-wheat" morphology, which consists of *c*-axis oriented aggregates of calcite rhombohedra.[201,205] Along these lines, spicule-like aggregates and hierarchically structured eight-pointed stars of calcite have also been reported at pH 10.5.[59,200]

In addition to calcite, aragonite and vaterite polymorphs can be grown in silica gels under conditions of high pH (8–10) and reactant concentration (supersaturation), using a double diffusion geometry.[200] Experimentally, the formation of vaterite spherulites was favored near the calcium reservoir, while spherulites of aragonite preferentially formed near the carbonate reservoir. Aragonite formation in silica gel at higher carbonate concentrations has also been achieved in silica gels that were formed at low pH (≈5.5).[202] These examples of aragonite formation under ambient conditions in the absence of additives clearly demonstrate the kinetic control afforded by hydrogel environments.

Coral-like aggregates of aragonite have also been formed in silica gel at high pH using a single diffusion method.[204] These aggregates were composed of plate-like subunits of aragonite that were enveloped by silica, pointing toward the potential of silica to behave as a chemically interacting medium at high pH. The self-organization mechanisms that underlie the formation of hierarchical structures in silica gel may stem from the experimental pH exceeding the pKa of the silanol groups in the hydrogel, thereby causing the gel to become an interacting medium. Further considerations regarding the observed morphologies include the possibility of (silica) gel incorporation during crystal growth, which was first observed in calcite even while the rhombohedral habit was preserved (see Section 4.3).[147]

Agarose hydrogels have also been used as a chemically inert matrix for the crystallization of calcium carbonate. Generally the calcite polymorph is obtained, although aragonite has been obtained by growth in agarose gels at elevated temperatures,[175] similar to results from solution-based experiments. Calcite crystals grown in agarose (1 w/v%) show a range of morphologies as a function of solute concentration (supersaturation), ranging from equilibrium rhombohedra to hopper-like 8-pointed stars (**Figure 9**a).[175] In general, the hopper- or skeletal-like crystals are formed at higher driving forces obtained by changing the calcium concentration or carbonate reactant source.[3,62,175] In addition, under certain conditions, the calcite crystals are found to incorporate the gel medium during growth to form organic-inorganic composite single-crystals (see Section 4.3).[173] Hierarchically-structured calcite has also been grown in 2 wt% agar gels.[62] These crystals, which had a rhombohedral macroscopic morphology that was composed of rhombohedral subunits, represent a shift towards a self-organization mechanism facilitated by the higher supersaturation present in denser gel media.[224]

Introduction of cationic additives. As "chemically inert" crystal growth media, silica and agarose hydrogels present opportunities to study the chemical effects of soluble additives on calcium carbonate crystallization, in particular on polymorph selectivity and crystal morphology. The crystals formed in the presence of additives reflect changes to the growth mechanism(s) caused by impurity incorporations: modifying growth steps or changing solubility (and thus supersaturation).[120] While some studies have used carboxylic acid or polysaccharide additives in gels,[180,181] most have focused on cationic additives, due to the known correlation of Mg^{2+} with the aragonite polymorph and

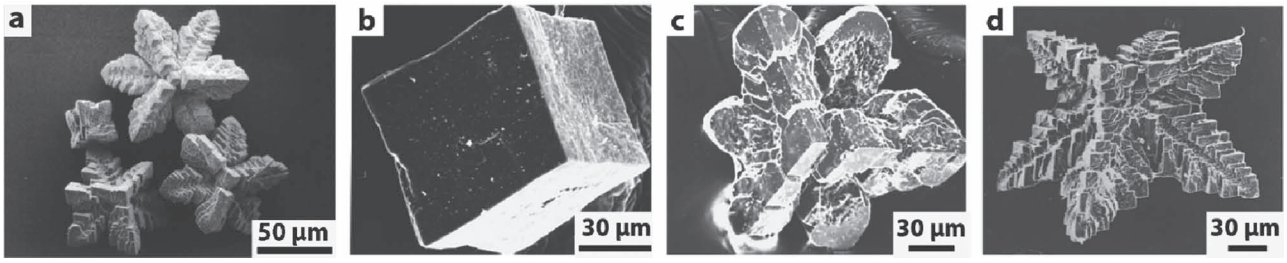

Figure 9. a) SEM images of 8-pointed calcite stars grown in 1 (w/w%) agarose hydrogel with no additives. b–d) Morphological evolution of calcite grown in 0.3% agar in the presence of variable radii impurity cations imaged by SEM: b) Ag^{+} (r = 115 pm), c) Cr^{3+} (r = 61.5 pm), and d) Al^{3+} (r = 53.5 pm) (Note: ionic radius of Ca^{2+} is 100 pm). Panel (a) adapted with permission.[175] Copyright 2003, Royal Society of Chemistry. Panels (b–d) adapted with permission.[179] Copyright 1998, Elsevier.

the anomalously high magnesium content found in some biological calcites.[225]

Introduction of cationic additives into double diffusion systems has been approached in different ways: loading of impurities into the gel itself, or by addition of the cationic impurity to the calcium reservoir. In most silica gel studies, impurities were added to the silicate solution before gelation to obtain an initially homogeneous distribution of impurity cations throughout the gel.[200] In the agar studies, the impurity cations were added to the calcium reservoir. The approach of loading impurity cations into only one region of the double diffusion system will result in impurity gradients. In addition, the two different loading procedures listed here will certainly have different effects on the solute diffusion gradients within the respective systems. These relatively unexplored considerations present opportunities for future studies on crystal growth in gels with additives.

In spite of the experimental complexities associated with crystallization studies in gels with additives some important relationships have been reported. At pH 5.5, calcite was precipitated under double diffusion in magnesium-loaded silica gels.[202] In this work, the concentrations of reactants along the gel column were determined at the time nucleation was first visible in the gel so that the supersaturation threshold could be monitored along the entire length of the gel column. The presence of magnesium in the gel media was found to increase the threshold supersaturation required to nucleate calcite, meaning that magnesium serves as an inhibitor to calcite formation. Calcite morphology evolved along the length of the gel column during the reaction (**Figure 10**) consistent with the supersaturation gradient that was quantified along the column. Magnesium content in the final crystals was quantified by electron microprobe analysis showing greater Mg^{2+} incorporation under conditions of higher supersaturation. Individual particles incorporated magnesium in zones, with the highest magnesium concentrations (up to 15 mol%) in the core. This zoning has also been observed with manganese substitution into calcite crystals grown in silica gels.[206] The morphologies of the magnesian calcites evolved from spherical aggregates (Figure 10a–d), formed at high supersaturation, to bundled sheafs at intermediate supersaturation (Figure 10e–g). Hopper-like morphologies formed in lower supersaturation regions were found to incorporate up to 7.5 mol% magnesium (Figure 10h).[202] These results illustrate a dependence of crystal morphology both on magnesium incorporation and on supersaturation, and may demonstrate that higher supersaturation can lead to greater impurity incorporation. While the individual connections from morphology to both supersaturation and magnesium content

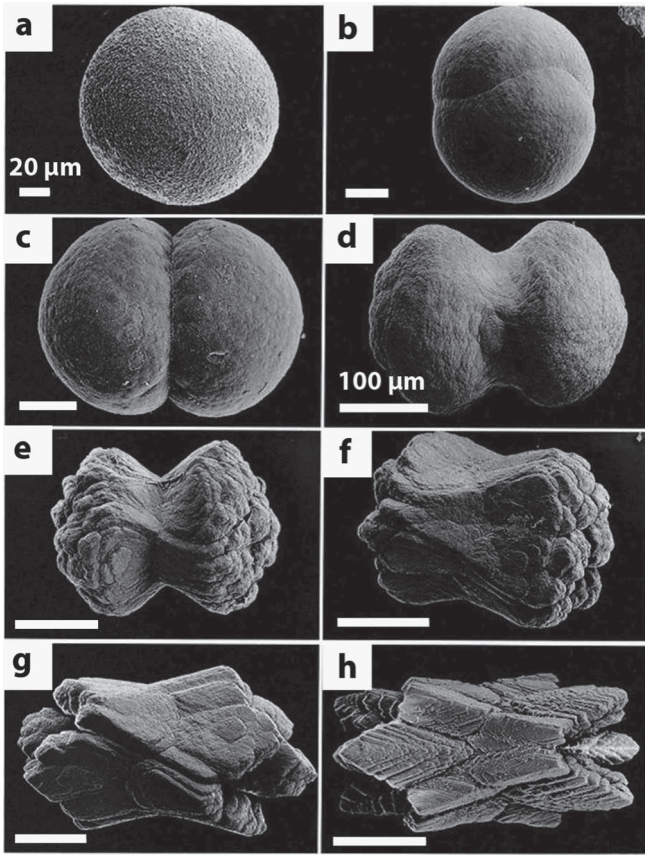

Figure 10. SEM images of calcite grown in silica gels under double diffusion. Morphology changes are linked to changes in magnesium content and supersaturation. The spherical aggregates shown in (a) contain the highest Mg^{2+} content and formed at the highest supersaturation. The supersaturation as well as the magnesium content of the crystallites decreases alphabetically to (h) where hopper-like morphologies formed at the lowest supersaturation and contain the lowest magnesium content. Scale bars (a–c) are 20 µm, (d–h) are 100 µm. Adapted with permission.[202] Copyright 1996, Geoscience World.

are well established, the relationship between impurity uptake (magnesium) and supersaturation is complicated. The relative contribution of each factor in determining the final morphology requires further investigation.

Other studies have expanded the range of cationic additives to include other alkaline earths as well as other metals, with both larger and smaller ionic radii than Ca^{2+} (Figure 9b–d).[179,203] Calcite crystals grown with substituted cations that have radii larger than calcium (e.g., Sr^{2+}: $r = 118$ pm) maintain a rhombohedral habit (Figure 10b), while those formed with cationic substituents with radii smaller than calcium (e.g., Co^{2+}: $r = 75$ pm) show a range of morphologies that depend on cationic additive concentration (Figure 10c,d). These results suggest a relationship between supersaturation and cation radius that is not yet well understood.

Finally, similar to solution growth, cationic additives in calcium carbonate crystallization have been found to strongly influence polymorph selection.[178,179,200,210] In silica gel, vaterite formation has been associated with the addition of Ba^{2+} and aragonite formation has been associated with the addition of Sr^{2+} and Ni^{2+}.[200] The formation of vaterite in agar gels has been observed with Ag^{+}, Al^{3+}, and Cr^{3+} impurities and displayed a dependence on concentration of the ionic additive.[179] In agar hydrogels, numerous divalent transition metal cationic additives have been shown to favor aragonite formation.[178] Aragonite can also be formed by additions of Ag^{+}, Al^{3+}, and Cr^{3+} impurities, with morphological variations that show a less clear dependence on the radius of the cations.[179]

4.2.2. Chemistry of the Hydrogel Affects the Local Crystallization Microenvironment

Hydrogels that contain charged and/or polar functional groups present a number of additional control variables for the growth of calcium carbonate crystals. First, these functional groups can interact with diffusing solutes (e.g., Ca^{2+}, CO_3^{2-}) to change the local concentration of reactants (supersaturation). Secondly, they can serve as nucleation sites to direct the orientation of crystals within the hydrogel network. Finally, some functional groups can interact directly with the growth steps and facets of the crystals themselves. In all cases, the presence of interacting chemical functionality within hydrogel matrices presents a means to study the chemical (as opposed to physical) effects on crystallization in organic matrices. Two examples of such hydrogels are gelatin, which contains both acidic (carboxylic acid) and basic (amine) groups, and polyacrylamide, which contains pendant amide groups.

Gelatin. When calcite is grown in 10 wt% gelatin hydrogels via double diffusion, spherulitic (polycrystalline) aggregates (100–400 μm diameter) of calcite form (**Figure 11**a)[145] In this work, the gelatin column was buffered to pH 8.35, the carbonate source was derived from sodium bicarbonate, and equimolar ratios of reactants were used. The appearance of the surfaces of the aggregates was found to vary as a function of position in the gel: particles formed closest to the Ca^{2+} source showed rough surface terraces, characteristic of formation under higher supersaturation, while those closest to the CO_3^{2-} source had smooth, faceted surface terraces, indicating formation at a lower supersaturation. The calcite aggregates were shown to incorporate ≈4 wt% of the gelatin matrix by thermogravimetric analysis (TGA). A radial internal microstructure was observed by optical cathodoluminescence that showed preferential incorporation of the gel into the core.[145] The spherical, aggregated morphology is generally indicative of formation under high supersaturation, and is quite similar to the spherulitic aggregates formed in silica gel with Mg^{2+} additives (Section 4.2.1, Figure 10b,c).[202] Interestingly, Fernández-Díaz et al. quantified a higher supersaturation nearest the carbonate reservoir in their silica hydrogel system, while Grassmann et al. used surface morphology to infer that the higher supersaturation was present at the calcium side of their gelatin system.

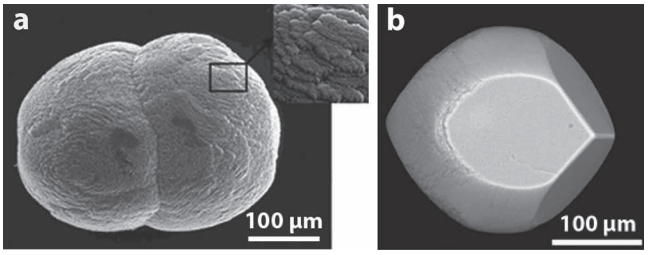

Figure 11. SEM images of calcite crystals grown in 10 wt% gelatin matrices under double diffusion: a) spherulitic aggregate formed with equimolar ratio of reactants ($CaCl_2$, $NaHCO_3$) and b) single crystal formed with 1:3 molar ratio of reactants ($CaCl_2$:Na_2CO_3). Panel (a) adapted with permission.[145] Copyright 2002, American Chemical Society. Panel (b) adapted with permission.[4] .

In a related study, single-crystal barrel-shaped calcite crystals (≈200 μm length) were formed closest to the calcium reservoir under double diffusion in 10 wt% gelatin gels (Figure 11b).[4] These crystals were also found to incorporate the gelatin fibers and to have a less-ordered and more porous central region by transmission electron microscopy (see Section 4.3).[164] In this work, the gelatin column was buffered to pH 7.4, the carbonate source was a sodium carbonate solution, and 1:3 molar ratio of calcium to carbonate was used. A comparison of the different morphologies formed under double diffusion in gelatin (Figure 11) and the poly- versus single-crystalline nature indicates that their formation took place under very different supersaturation conditions. These different growth environments could be caused by the different pH, or the absolute and relative concentration of reactants, as well as the different carbonate sources. Further experimentation is necessary to determine which factor(s) dominates the formation mechanism.

Polyacrylamide (PAA). Pseudo-octahedral crystalline aggregates of calcite with 150–250 μm diameter were grown by double diffusion in a buffered (pH 8.35), 10 wt% PAA hydrogel using an equimolar ratio of reactants (100 mM) (**Figure 12**a).[60] These calcite composites were shown to consist of oriented rhombohedral crystallites ≈5 μm in diameter, interspersed with the PAA hydrogel matrix (Figure 12b). It is worth noting that the morphology of the aggregates did not vary with position along the PAA gel column. Individual aggregates diffracted electrons as single crystals (inset, Figure 12b). The morphology of the calcite aggregates was found to depend on the concentration of PAA in the hydrogel matrix, forming rhombohedral aggregates in lower concentration PAA hydrogel systems.[19,99] Further, incorporation of the hydrogel matrix into the aggregates

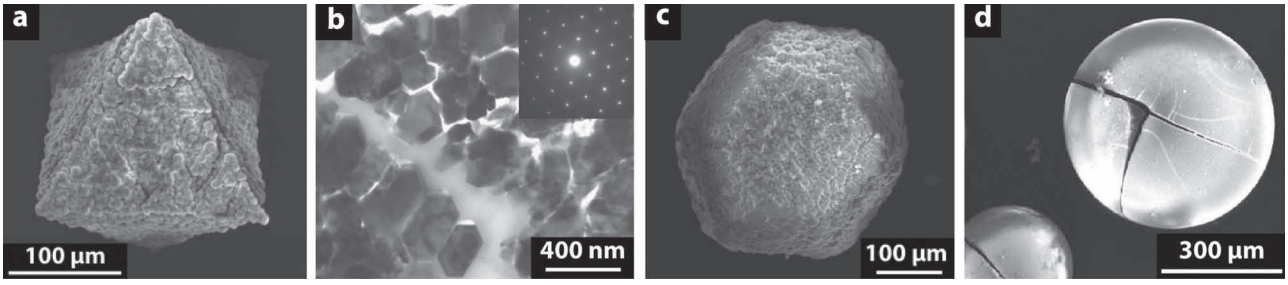

Figure 12. Pseudo-octahedral aggregates of calcite formed under double diffusion in 10 wt% polyacrylamide hydrogel: a) SEM image of pseudo-octahedral morphology; b) TEM image of aligned subunits with selected area electron diffraction inset showing single crystal characteristics of individual crystallites; and c) cuboctahedral aggregates formed in 10 mol% sulfonated PAA hydrogel; (d) calcite spherulites formed in 10 wt% carboxylated PAA hydrogel. Panels (a,b) adapted with permission.[60] Copyright 2003, Mineralogical Society of America. Panel (c) adapted with permission.[199] Panel (d) adapted with permission.[5] Copyright 2004, Elsevier.

was quantified by TGA. In a gel with ≈10 wt% polyacrylamide content, 0.7 mass% gel was incorporated within the composite products.[60] The assembly of rhombohedral subunits into pseudo-octahedral aggregates was speculated to result from a high heterogeneous nucleation rate in the PAA matrix caused by a high apparent supersaturation. In this scenario, the presence of numerous rhombohedral nuclei prevent classical ion-by-ion growth, and thus oriented assembly of these nuclei are driven by a reduction in surface energy, during which incorporation of the gel network occurs.[60]

4.2.3. Covalent Modification of Synthetic Hydrogels

In solution-based growth, the difference in function between soluble (free) and substrate-bound (immobile) additives is well-known. For example, small-molecule carboxylates in solution inhibit calcite growth,[226] whereas carboxylate functionalized surfaces can direct the oriented nucleation of calcite crystals.[227] Applying similar ideas to gel-growth becomes complicated: will a functional group covalently bound to the gel network behave more like a growth modifier (free in solution) or nucleation promoter (immobilized)? Based on the physical and chemical aspects of hydrogel matrices discussed above, covalent modification of synthetic hydrogel networks with acidic or basic species can be used to achieve refined control over the crystallization microenvironment.

Sulfonated Polyacrylamide (sPAA). Copolymerization of acrylamide with sulfonate-containing monomers[199] was used to introduce anionic functionality to a PAA hydrogel matrix, consistent with the sulfonated polysaccharides found in some biomineralization systems.[155] The negatively charged sulfonate groups were chosen for their potential to interact with calcium cations to change the local chemical environment and thereby the growth rate. In addition, the sulfonate functionality has the potential to interact with growing crystal surfaces or act as nucleation sites.

Similar to the pseudo-octahedral calcite aggregates formed in pure PAA, calcium carbonate crystallization in sPAA with equimolar ratio of reactants forms aggregates of calcite with internal architectures composed of rhombohedral subunits.[199] While pseudo-octahedral aggregates were formed in native PAA, the external morphology of the aggregates formed in sPAA showed cuboctahedral symmetry (Figure 12c). The cuboctahedral morphology was observed along the entire length of the sPAA hydrogel column, but the size of these aggregates varied; from 100 μm near the calcium reservoir to 500 μm near the carbonate reservoir. The morphology of the aggregates was seen to change as a function of sulfonate content, proceeding from pseudo-octahedral aggregates (native PAA) to cuboctahedral aggregates at 10 mol% sulfonate via flattening of the pseudo-octahedral faces. While the aggregation-based growth model in PAA gels appeared to be maintained in the presence of sulfonate functionalities, the change in morphology suggests a role for the sulfonate groups in modifying the relative growth rates of the individual faces of the rhombohedral subunits.[199] While the similarity in proposed growth mechanism in sPAA as compared to native PAA suggests that matrix incorporation might occur, the incorporation of organic material was not monitored, so the effect of sulfonate functionality on matrix incorporation is yet to be determined.

Carboxylated Polyacrylamide (cPAA). Similar to the sPAA discussed above, copolymerization of polyacrylamide hydrogels with carboxylate groups (acrylic acid)[5] was used to model the Asp- and Glu-rich proteins found in many biogenic matrices.[155] In contrast to native PAA and sPAA gels, calcium carbonate crystallization in these cPAA gels proceeded much slower and formed polymorphs and morphologies that evolved with time. After seven days under double diffusion with equimolar ratio of reactants (100 mM), a mix of vaterite spheres and calcite rhombohedra (less than 5 μm) were observed. These products exhibited no visible changes for an additional seven days. After twenty-eight days only spherical aggregates of calcite (300 μm) remained (Figure 12d). Thermogravimetric analysis was used to determine that these calcite aggregates contained 4.2 mass% (9 vol%) of the cPAA hydrogel network. Further analysis of the calcite aggregates showed a spherulitic microstructure, and conchoidal fracture, implying that they had formed rapidly from a central seed.

The significant differences in both the crystallization process and final morphology of crystals formed in cPAA as compared to native PAA and sPAA imply that a different growth mechanism governs their formation. The initially suppressed nucleation is consistent with the inhibitory effects of polyacrylic acid on calcium carbonate crystallization.[182] The formation of vaterite is consistent with kinetic stabilization of this less stable polymorph by the carboxylate groups.[5] The spherulitic

character of the final aggregates as well as the delay in their formation indicates an induction period during which high supersaturations develop to facilitate the rapid growth mechanisms responsible for this morphology. Matrix incorporation may occur during this period of rapid growth or during ripening to the final morphology.

4.2.4. "Designer" Hydrogels

More recently, small-molecule hydrogels have been designed to serve as biomimetic organic matrices for crystallization. For example, carboxylic acid functionalities have been introduced into a bis-urea hydrogel system to interact with calcium ions.[146] The morphology of calcite crystals grown in these gels evolved over time, initially growing as rhombohedral crystals that, with time, first developed etch pits and subsequently, irregular overgrowth structures. Etching studies performed on the initial, as-grown rhombohedral crystals resulted in non-regular and deep etch pits, suggesting the non-specific incorporation of gelator molecules into the crystals (Section 4.3). In other work, calcite was grown using a supramolecular gel composed of *N,N′,N″*-tris(3-pyridyl)-trimesic amide.[214] In contrast to most biomimetic approaches, this hydrogel was designed to interact with carbonate anions through the presence of amide and pyridyl functional groups. Similar utilization of positively charged additives to the calcium carbonate crystallization media is still relatively new in solution studies.[228] Calcite crystals grown in this fibrous gel were shown to grow around whole fibers (500–1000 nm in diameter).[214] These studies and others support the idea that synthetic matrices can be designed to interact specifically with either the ionic species during nucleation or with the growing crystals to direct growth and final morphology.

4.3. Incorporation of the Gel-Matrix During Crystal Growth

One of the outstanding questions in biomineralization is how large calcite single crystals can incorporate organic macromolecules while still diffracting X-rays and/or electron beams as single-crystals. Although the incorporation phenomenon in both biogenic[57,149,229–232] and synthetic[58,233–243] crystals has been widely addressed and studied, the incorporation mechanism(s) is still poorly understood.[3,243] Crystal growth in gels provides ideal platforms with which to study this phenomenon since several types of gel-grown crystals have been identified that incorporate the gel media and become gel/single-crystal composites.

Although the examples of gel-incorporated crystals are limited, as compared with the large number of gel-grown crystals, the types of gel-incorporated crystals are diverse, including crystals of inorganics and organics, small molecules and macromolecules. Initially, in 1969, Nickl and Henisch reported that calcite crystals grown from silica gels incorporated the silica matrix.[147] Subsequently, García-Ruiz et al. found that gel-grown protein (lysozyme, ferritin and thaumatin) crystals can incorporate the gel (silica and/or agarose) matrix.[123,148] We have demonstrated that calcite, α-glycine, and calcium tartrate tetrahydrate crystals grown in agarose gels incorporate the polymer network, and that the crystals maintain their long-range order (single-crystal nature).[3,58,173,244]

In other work, Huang et al. showed that calcite crystals grown in gelatin gels also incorporate the gel material.[4,164] The barrel-shaped crystallites obtained by Huang et al. (Figure 11b) diffracted X-rays as single crystals. These crystals were seen to have a less-ordered and more porous central region by transmission electron microscopy, consistent with the different structural regions of in vivo otoconia (Figure 5). Matrix incorporation was attributed to high supersaturation conditions, which resulted from the interaction of ionic carboxylate groups on Asp and Glu residues in the gelatin with calcium ions thereby forming a specific microenvironment for crystal growth.[145] Huang et al. extended this work by modifying the gelatin media to more closely resemble an otoconia-like glycoprotein matrix by including agar as a polysaccharide source.[4] The morphology of crystals became more elongated with well-defined faceted ends, and more closely resembled human otoconia.

4.3.1. Possible Incorporation Mechanisms

Before gel-incorporation was first reported by Nickl and Henisch, Khaimov-Mal'kov had proposed that a growing crystal exerts a crystallization pressure on the surrounding gel media.[245] His work suggested that whether or not the crystal incorporated the gel was determined by whether or not the gel was strong enough to resist the crystallization pressure. If the gel network were strong, then the crystal would grow around it, whereas if it were weak, it would be broken or pushed away. Indeed, "cusps" in gel are often observed at the corners and edges of the growing crystals where the gel has been disrupted.[246,247] Following Khaimov-Mal'kov's hypothesis, Gavira and García-Ruiz calculated the magnitude of the crystallization pressure from growing protein crystals on agarose gel networks and found that the pressure was much higher than the gel strengths, suggesting that the crystals would always break or push away the gel media.[148] In their experiments, however, the pressure did not disrupt the gel as expected and the authors only obtained crystals with gel-incorporation. The discrepancy between the calculation and the experimental results implies that the competition between gel strength and crystallization pressure at the growth front is not the only factor determining the incorporation of gel matrix.

The crystal growth rate is another possible variable that is important for determining incorporation of the gel matrix. It is well-known that at faster growth rates, crystals incorporate larger amounts of atomic or small molecule impurities.[202] A similar kinetic effect has also been observed for the incorporation of micrometer-sized particles into crystals: at slow growth rates, growing crystals do not incorporate the particles, but once the growth rate increases beyond a critical value, incorporation of particles takes place.[248–250]

4.3.2. Experiments: Calcite Crystals Grown in Agarose Hydrogels

We have recently worked to understand the many factors leading to gel-incorporation during crystal growth, in particular, the interplay between crystal growth rate and gel strength on gel-incorporation. For this work, we have focused on the growth of calcite crystals in agarose hydrogels as a model system.[3,173,244] As discussed in Section 4.2.1, calcite growth in

agarose can yield a range of morphologies from well-formed rhombohedra to hopper- or skeletal-like crystals. Results from our lab have revealed that calcite crystals grown in agarose hydrogels incorporate gel fibers uniformly without disrupting the rhombohedral morphology or crystallography of calcite crystals (**Figure 13**a). After gentle etching of the crystals in deionized (DI) water, the incorporated gel fibers emerge from the crystal (Figure 13b). To observe the incorporated fibers in situ, we have examined the internal structure of gel-grown calcite crystals by annular dark field scanning transmission electron microscopy (ADF-STEM) and electron tomography. These images reveal a network of gel fibers laced throughout the crystal (Figure 13c).[58] Higher magnification images reveal that the crystal uses both high- and low-energy facets to accommodate the gel's tortuous structure (Figure 13d,e). Selected area electron diffraction (SAED) demonstrates that despite the presence of the gel fibers, the single crystal nature of the calcite is not disrupted (Figure 13d inset).

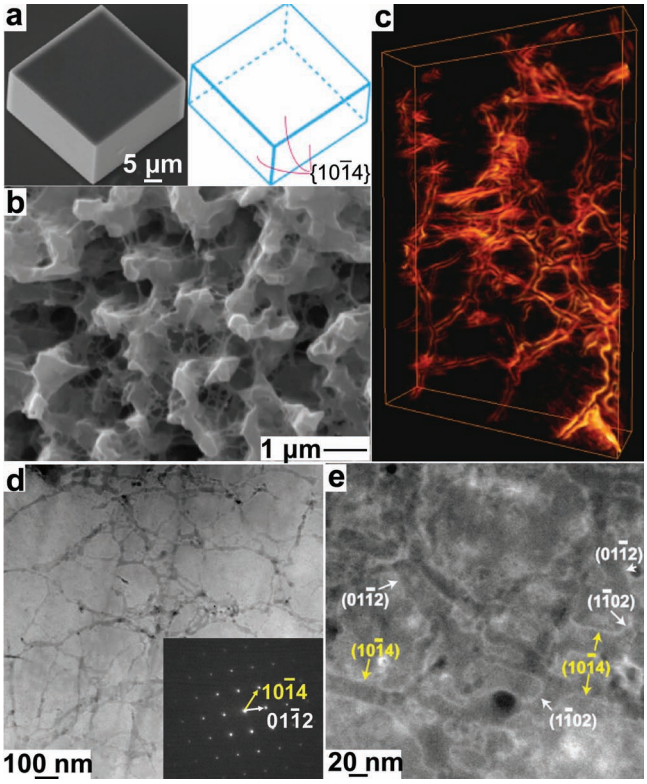

Figure 13. Structural characterization of porous single crystal calcite agarose composites: a) a SEM image of a single calcite rhombohedron and a model of a calcite crystal expressed by six {10$\bar{1}$4} faces; b) a SEM image of a gel-grown calcite crystal after etching in DI water for 4 days, showing the exposed incorporated gel fibers; c) electron tomography reconstruction of the randomly distributed agarose network inside a section of calcite single crystal; and d,e) porous internal structure shown by ADF-STEM. Interfaces between the crystal and fibers are partially indexed. For clarity, faces in the {10$\bar{1}$4} family are indicated in yellow, whereas faces in the {01$\bar{1}$2} family are highlighted in white. Inset in (d): a SAED pattern showing single crystal nature. Panels (a,c,d,e) adapted with permission.[58] Copyright 2009, AAAS. Panel (b) adapted with permission.[173] Copyright 2007, Royal Society of Chemistry.

More recently, we have investigated the factors relevant to gel-incorporation.[3] We predicted, based upon Khaimov-Mal'kov's work,[245] that for a given crystallization pressure (thermodynamic driving force) there should be a "threshold" gel strength at which gel-grown crystals should switch from no incorporation to complete incorporation. Similarly, for a given gel, there should be a critical growth rate at which incorporation begins to occur. Until now, this kind of transition, however, has not been demonstrated experimentally for a single gel-crystal pair. We designed a set of experiments to systematically examine the effects of gel strength and crystal growth rate on gel-incorporation. To change the growth rate, we varied Ca^{2+} concentration. Because we were using the gas diffusion (ammonium carbonate) method[251] to grow the crystals (Figure 2b), the carbonate concentration is continuously evolving throughout the experiment, and so we cannot define an absolute supersaturation in the gel. Qualitatively, increasing Ca^{2+} concentration leads to an increase in growth rate, as suggested by the crystal morphology evolution (**Figure 14**a insets). To change the gel strength, we looked at growth in two different commercially available agarose types with different degrees of hydroxyethylation, agarose 1B (high strength) and agarose IX (low strength), both from Sigma-Aldrich. As the degree of hydroxyethylation increases, the gel strength decreases due to disruption of the hydrogen bonding network.[3,82,84] We then studied how agarose incorporation varied as a function of calcium and gel concentration in both of these gels. Increasing the agarose concentration in the gels is also a way of changing the gel strength since it leads to denser, cohesive interactions (e.g., hydrogen bonding) among agarose chains and, thus, higher gel strength.[85]

Effects of growth rate ([Ca^{2+}]) on gel-incorporation. Calcite crystals were grown in agarose hydrogels containing a range of concentrations of $CaCl_2$ ([$CaCl_2$]). In both agarose 1B and agarose IX, at low [$CaCl_2$], the crystals exhibit the characteristic rhombohedral morphology of calcite expressed by six {10$\bar{1}$4} faces (Figure 14a,b, insets). With increasing [$CaCl_2$] in both gel types, the crystal morphology gradually evolves into "hopper-like" shapes (Figure 14a,b insets), suggesting 2D nucleation is taking place at the corners and edges of the crystals.[2,119] The observation of such crystal morphologies is consistent with diffusion-limited growth and faster growth rates, as would be expected at higher [$CaCl_2$].

To quantify the amount of incorporated agarose, the gel-grown crystals were examined by thermogravimetric analysis (TGA).[3] In both gels, at higher [$CaCl_2$] (faster growth rates), the amount of incorporated material reaches a plateau, or saturation level (Figure 14a,b). The saturation values are close to the calculated value (≈0.3%) for crystals incorporating all of the agarose fibers they encounter, as well as some amount of water.[3] In agarose IX, at low [$CaCl_2$] (slow growth rates), TGA of the crystals shows no appreciable weight loss (Figure 14b). In contrast, in agarose 1B at low [$CaCl_2$], incorporation is still observed, just at a lower level than the saturation amount. It is possible that for agarose 1B, we did not achieve slow enough growth rates to observe no incorporation in this stronger gel. Alternatively, differences in the gel chemistry may lead to different strength interactions between the gel and the growing crystals, which in turn lead to different amounts of incorporation.

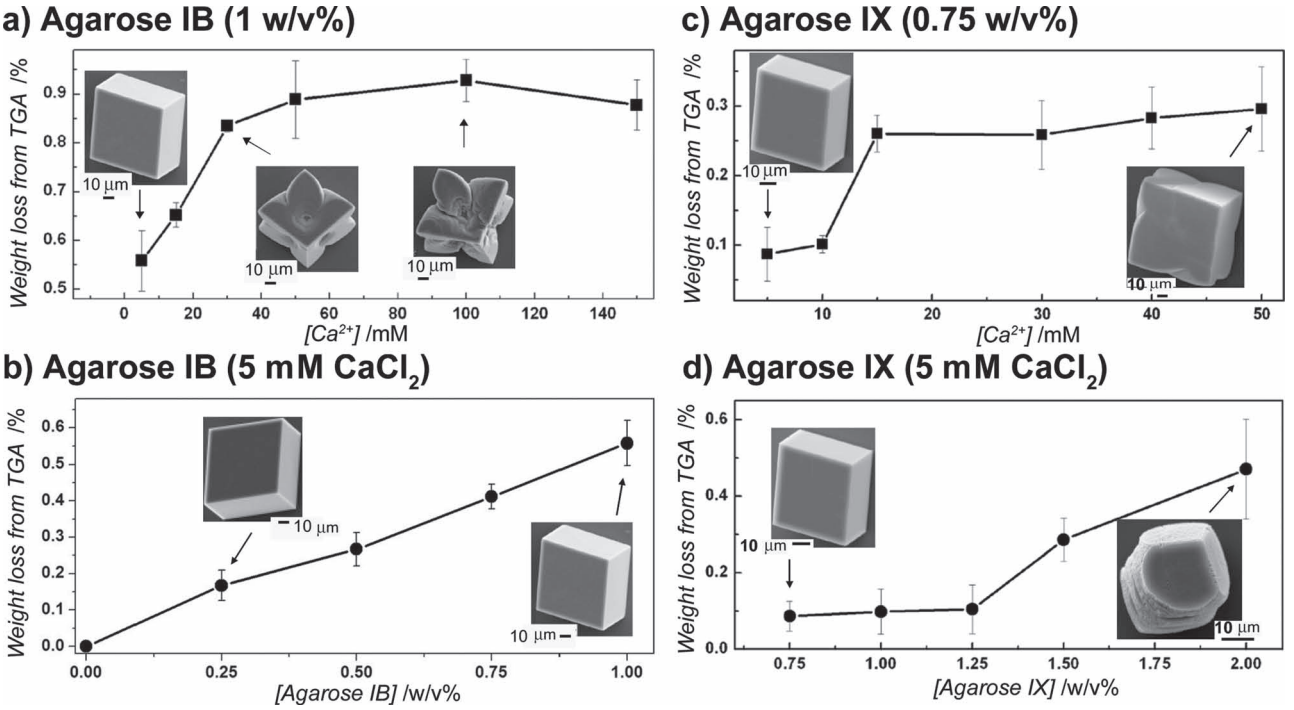

Figure 14. The weight loss above 150 °C calculated from TGA analyses for the calcite single crystals grown under systematically varied conditions: a) different $CaCl_2$ concentrations in a gel (1 w/v% Agarose IB), b) different $CaCl_2$ concentrations in a gel (0.75 w/v% Agarose IX), c) different gel (Agarose IB) concentrations with a fixed $CaCl_2$ concentration (5 mM), and d) different gel (Agarose IX) concentrations with a fixed $CaCl_2$ concentration (5 mM). Insets: Representative SEM images of calcite crystals grown under the conditions indicated by the arrows. Panels (a,b) adapated with permission.[3]

Effects of gel strength on gel-incorporation. Comparison of the above results for agarose 1B and agarose IX at the low [$CaCl_2$] already provides insight into a possible role for gel strength in determining incorporation. At the slow growth rates, there is no incorporation observed for the weaker of the two gels (agarose IX). This observation is consistent with Khaimov-Mal'kov's prediction,[245] however, since we are changing slightly the chemical structure of the gel, it is possible that changes in the gel-crystal interaction are responsible for the change in incorporation.

To further examine the role of gel strength, we examined calcite crystals grown in both types of agarose hydrogels with a fixed [$CaCl_2$] (5 mM), but different gel concentrations. The crystal morphology does not change significantly with increasing gel concentration in agarose IB (Figure 14c).[3] In agarose IX, however, at higher gel concentrations the crystals develop curved surfaces at the corners (Figure 14d, insets). This change in morphology is possibly due to specific agarose-crystal interactions.

TGA was again used to determine the amount of incorporated organic material. For agarose 1B, the amount of gel incorporated increases approximately linearly with increasing gel concentration (Figure 14c).[3] In contrast, for agarose IX, the dependence of the amount of incorporated agarose on gel concentration is nonlinear (Figure 14d). At lower gel concentrations (lower gel strength), TGA shows negligible weight loss. At higher gel concentrations, the amount of incorporation begins to increase as a function of gel concentration. In addition to changing gel strength, changing the gel concentration also will affect the gel structure (e.g., pore size) and possibly the supersaturation within the gel. Further experiments are required to fully deconvolute the contributions of all of these factors.

4.3.3. Proposed Mechanism for Gel-Incorporation: Competition at the Growth Fronts

By examining a range of growth conditions and gels, we have gained further insight into the variables that determine the amount of gel incorporation observed in a given system. We have observed three main regimes: 1) no incorporation at slower growth rates in a weaker gel; 2) partial incorporation at slower growth rates in a stronger gel; and 3) complete incorporation at faster growth rates in both weaker and stronger gels (**Figure 15**). The transition of crystals between these three states suggests that competing factors favor and disfavor gel-incorporation and that these competing factors are dependent on crystal growth rate and gel strength. Increasing both growth rate and gel strength favors gel-incorporation. The effect of growth rate on gel-incorporation is consistent with the force competition model previously suggested by Chernov and Temkin[248,252] for crystallization in the presence of particles.[248–250] The effect of gel strength on gel-incorporation verifies the importance of gel resistance to the crystallization pressure proposed by Khaimov-Mal'kov.[245]

As a growing crystal approaches a gel fiber with poor mutual wetting at the growth front, there is a force competition between a "disjoining force," a hydrodynamic force, and the resistance of the gel network (**Figure 16**a).[245,248,252] Chernov first described

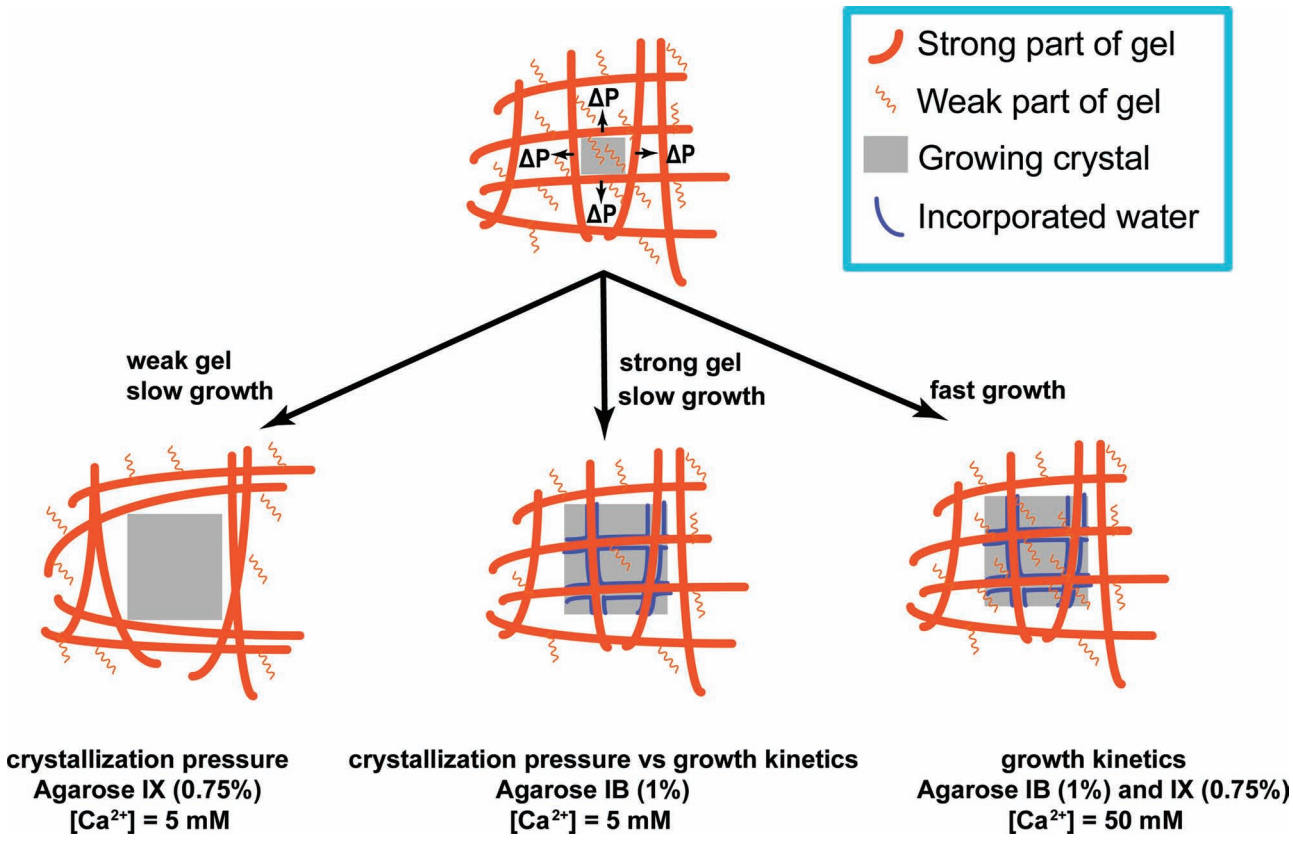

Figure 15. The proposed mechanism for agarose matrix incorporation during calcite crystal growth: a balance between the resistance of the gel fibers to crystallization pressure and the growth rate. Depending on the experimental parameters, either crystallization pressure or growth rate dominates and the resulting crystals are either pure single-crystals or single-crystals with completely incorporated gel fibers, respectively. In intermediate cases, crystals will partially incorporate the gel network. For further details, see the text. Adapated with permission.[3]

and defined the "disjoining force" as originating from repulsive van der Waals forces at the interface between a growing crystal and a foreign object.[119] In our case, the tendency of the disjoining force to push the fibers away from the crystal is equivalent to a reduction in the chemical potential of the liquid film between the crystal and the fiber as compared to that of the bulk liquid. For further discussion of the disjoining force, see ref. [[119,239,245]] The disjoining force disfavors incorporation of the gel fiber by the growing crystal, while the hydrodynamic force and the resistance of the gel network favor it. The hydrodynamic force is proportional to the crystal growth rate and the resistance of the gel network increases with gel strength. When growth rate or gel strength is high enough, the cooperation of the hydrodynamic force and the resistance of gel network will counteract the disjoining force and the gel fibers will be incorporated. Otherwise, the disjoining force will overcome the combination of the other two and the gel fibers will be pushed away.

In addition to the force competition, we suggest that there is also a mass competition (Figure 16b).[119] As first suggested for particles by Chernov, the agarose fibers screen the growth fronts beneath them from mass transport so that these growth fronts have higher transport resistance than the nearby growth fronts that are free of screening. Both the screened (Figure 16b, green "brick") and unscreened (Figure 16b, blue "brick") growth fronts advance, competing for "nutrients". Crystal growth at the screened growth fronts near the fiber disfavors gel-incorporation, while growth at the unscreened growth front favors it. The faster the growth rate, the higher the transport resistance for the screened growth fronts because less time is allowed for ions to diffuse into the gap between the growth front and the fiber. Therefore, higher growth rates favor gel-incorporation because of this mass competition.

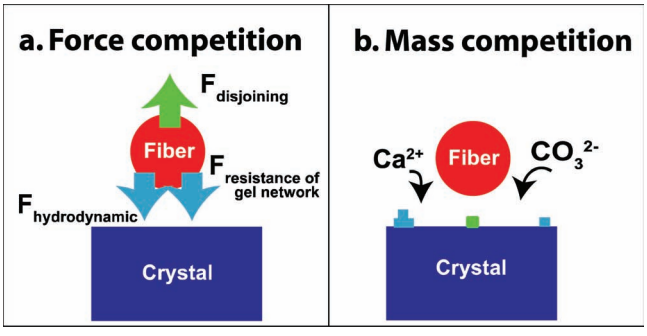

Figure 16. A schematic representation of the proposed gel-incorporation mechanism with a) a force competition and b) a mass competition at the growth front nearby an agarose gel fiber. For further details, see the text.

To summarize, for the calcite-agarose system, the two key variables for controlling gel incorporation are: 1) growth rate and 2) gel strength. While increased gel incorporation was found with increasing gel concentration, it is not clear if the changes to morphology were a result of the amount of incorporated gel or simply a result of changes to the growth rate caused by changes in the local chemical environment. The next step is to determine the generality of these "rules" for other gel-crystal pairs: first, for chemically "non-interacting" gels and then for gels that have the capability to strongly interact with the growing crystals. By understanding the interplay of physical and chemical effects on gel-incorporation, researchers will be able to determine design criteria for the pairing of host crystals with gels to achieve the desired degree of inclusion, and potentially thus tailor the mechanical properties of the resulting composite crystals.[243]

5. Summary and Outlook

The common theme of crystal growth in gels presented by matrix-mediated biomineralization systems provides a technique to investigate the mechanisms that govern composite formation in biogenic systems. As a medium for crystal growth, hydrogel networks maintain diffusion-limited growth conditions, which can be used to achieve a wide range of morphologies and architectural arrangements in the final crystalline products. The chemical functionality and microstructure of hydrogels varies amongst gel types and with gel concentration and provides a means to tune the kinetic variables of the growth rate and supersaturation in the crystallization microenvironment. A summary of calcium carbonate products obtained from growth in hydrogels is compiled in Table 2.

Crystallization of calcium carbonate in gels has elucidated some of the underlying effects that may govern the formation of complex mineral structures in biogenic systems. First, the observed morphology and polymorph appears largely to be a consequence of the growth mechanism as determined by the supersaturation. The supersaturation in turn, is dictated by the local chemical environment, which depends on the chemical functional groups present in the matrix itself. Further, the local chemical environment in gels varies with the gel concentration due to changes in the pore sizes and microstructure of the gels. Moreover, organic matrix incorporation during crystal growth depends on the gel strength and concentration, and the growth rate.

At this point, it is an interesting exercise to look at the similarities and differences in products from among the gel types discussed. There are three main types of calcite structures that form: 1) single crystals, with and without incorporated matrix, which have been reported to form in silica, agarose, and gelatin gels; 2) pseudo-single crystal aggregates, which have been reported to form in native PAA, sPAA, and agar gels; and 3) polycrystalline, spherulitic aggregates, which have been reported in silica, gelatin, silk, and cPAA gels. Since all of these experiments have been performed over many years and by many different labs, there is significant variation in the reaction conditions (e.g., pH, reactant concentrations and ratios, gel length and diameter), making direct comparisons among gels nearly impossible. Several interesting trends, however, can still be identified. First, single crystals are most commonly reported in the two "non-interacting" gels, silica and agarose. This result strengthens the assignment of these gels as relatively, chemically inert towards calcite. Second, the observation that multiple morphologies can be observed within the same gel-type (e.g., there are reports of both single crystals and polycrystalline spherulites in gelatin and silica gels) emphasizes the importance of growth conditions, and most likely supersaturation, on the final structure.

In those cases where care has been taken to maintain consistent conditions across gel types,[5,60,145,199] further conclusions can be drawn. For example, the striking differences observed by Grassmann and Lobmann between the pseudo-single crystal aggregates obtained in PAA and sPAA (Figure 12) and the spherulites from gelatin (Figure 11a) and cPAA (Figure 12d) imply that the chemistry and physical properties of the matrix do affect growth. It is difficult, however, even within this set of data to determine which characteristics of the matrix play the largest role in defining the product morphology. For example, one possible interpretation is that the ionic groups within gelatin and cPAA lead to the polycrystalline spherulites by locally sequestering calcium and thus increasing the supersaturation. Spherulitic structures, however, are also observed in silica gel in the presence of Mg^{2+} or at a high pH. As is true for solution growth studies, therefore, it is important to remember that just because two crystals look like each other, does not mean that they formed via the same mechanism or as a result of the same types of interactions. Our hope for the future is that research will be aimed at merging these seemingly disparate works into a unified map for understanding the formation of complex, crystalline structures in gels.

In order to grow a variety of materials (i.e., beyond calcium carbonate) in hydrogels to obtain organic-inorganic composites for a range of applications, it is important to establish the relationship between growth conditions, hydrogel choice, and the amount of incorporated organic material and the final crystal morphology. As this area of research continues to grow, we anticipate that the use of "designer" gels with tailored chemical functionality, such as peptides derived from proteins involved in biomineralization, will become increasingly important. The presence of functionalized substrates coupled with hydrogel media[169,244] can also impart another level of control, particularly over nucleation. Ultimately, this field should strive to determine design criteria for the pairing of host crystals with hydrogels to achieve the desired structure for a given application. Regardless, as discussed in this article, crystal growth in gels has already established itself as a member of the 'bio-inspired crystallization toolbox' alongside small-molecule and polymeric additives.[7,224,253,254] As we, as a community, move beyond the phenomenological treatment of growth in hydrogels to a fully developed understanding of the crystal growth mechanisms in such environments, we will enable the synthesis of complex, hierarchical, single-crystal composites with tunable physical properties.

6. Experimental Section

Hydrogel Preparation for Imaging (Figure 1): Silk: Silk fibroin was obtained from *Bombyx mori* (silkworm) cocoons. The cocoon material

was boiled in one of the following solutions: 1) 5 w/v% Marseilles soap solution (an olive oil based soap from Marseilles, France),[218] or 2) 0.02 M sodium carbonate (Na_2CO_3, J.T. Baker) for 2 h,[90] changing the solution every 15 min to solubilize and remove the silk sericin. After boiling, the silk was rinsed with copious amounts of water to remove excess salts or surfactants. The resulting silk mass was dissolved overnight, at room temperature, in 9.3 M lithium bromide (LiBr, Reagent Plus ≥99%, Sigma-Aldrich). The solubilized silk was then filtered and dialyzed (Slide-a-Lyzer dialysis cassettes, Pierce, MWCO 3,500)) for three days. Fresh aqueous silk solutions (3 mL), in capped glass test tubes were incubated in a hot water bath at 60 °C. Hydrogels formed from Marseilles soap purified silk fibroin gelled in 2 days; those purified with sodium bicarbonate took 4 days to gel.

Silica: Aqueous solutions (0.5 M) of sodium metasilicate nonahydrate (Sigma-Aldrich) were gelled by additions of equal volumes of diluted hydrochloric acid (Fisher Scientific). Basic gels (final pH ≈9) were formed using 1 M hydrochloric acid, and acidic gels (final pH≈2) were formed using 2 M hydrochloric acid. Solutions were allowed to gel in sealed scintillation vials in a water bath at 30 °C. Gel times varied depending on pH, with acidic gels taking 4 weeks to gel and basic gels taking less than 1 h.

Freeze-Drying: All hydrogel samples (≈1 mL) were frozen in liquid nitrogen and placed on a lyophilizer for 18 h. Freeze-dried hydrogel samples were sputter-coated with carbon using a rotating, tilting stage. Subsequently, samples were sputter-coated with Au/Pd. Scanning electron microscopy (STEREOSCAN 440 LEICA, 20 kV) was used to image the microstructures of the gel networks.

Crystal Growth Experiments: Experiments in Agarose IB were previously reported.[3] For Agarose IX, agarose solutions (0.75–2 w/v%) were prepared by dissolving agarose powder (Type IX, Sigma, gel point: 8-17 °C) in a hot solution of 5-50 mM $CaCl_2$•$2H_2O$ (99+%, Sigma-Aldrich). The warm agarose solution (3 mL) was filtered (syringe filter; 0.2 µm, Nylon, Millipore) into a Petri dish (35 mm × 10 mm) that was then cooled in a refrigerator (about 0 °C) for gelation (30 min) and equilibrated at ambient temperature for another 30 min. After gelation, the Petri dishes were covered with aluminum foil with one small hole.

The Petri dishes with the gels were placed in a closed desiccator containing one vial of ammonium carbonate (Sigma-Aldrich). After 48 h in the desiccator, crystals grew in the bulk gels and were removed from the gels by dissolving the agarose in boiling deionized (DI) water (18.2 MΩ, Barnstead EASYpure RoDI) for three times. The obtained crystals were then rinsed with DI water and ethanol.

Characterization of Calcite Crystals: The morphologies of the crystals were examined by scanning electron microscopy (STEREOSCAN 440, LEICA, 25 kV, 600 pA) after being sputter-coated with Au/Pd. Thermogravimetric analysis (TGA) of the crystals was conducted with a thermogravimetric analyzer (TA Instruments Q500) under a flowing air atmosphere and with a heating rate of 5 °C per minute from ambient temperature to 450 °C. Ten to twenty milligrams of crystals were used for each run after drying overnight in oven (≈80 °C). Each TGA experiment was repeated 3 times. TGA of geological calcite (calcite Iceland spar, Carolina Biological) was used as a control.

Acknowledgements

E.A.-S. and H.Y.L. contributed equally to this work. L.A.E. acknowledges support from NSF (DMR 0845212), the Cornell Center for Materials Research (CCMR), a Materials Research Science and Engineering Center of the NSF (DMR 1120296), the J.D. Watson Investigator Program (NYSTAR contract no. C050017), and the Cornell Engineering Learning Initiatives (ELI). In addition, E.A.-S. acknowledges support from NSF Graduate Research Fellowship (DGE-0707428) and Integrative Graduate Education and Research Traineeship (DGE-0903653) Programs. Particular acknowledgement is made of the use of the shared facilities at CCMR (DMR 1120296). The authors thank Prof. Guiseppe Falini for kindly providing high-resolution images for Figures 6 and 8. Finally, the authors thank all of their lab members and colleagues who over the years have contributed to their understanding of crystal growth in gels.

Received: January 31, 2012
Published online: May 3, 2012

[1] F. Lefaucheux, M. C. Robert, in *Handbook of Crystal Growth*, Vol. *2* (Ed: D. T. J. Hurle), Elsevier Science, Amsterdam **1994**.
[2] H. K. Henisch, *Crystal Growth in Gels and Liesegang Rings*, Cambridge University Press, Cambridge **1988**.
[3] H. Y. Li, L. A. Estroff, *Adv. Mater.* **2009**, *21*, 470.
[4] Y. X. Huang, J. Buder, R. Cardoso-Gil, Y. Prots, W. Carrillo-Cabrera, P. Simon, R. Kniep, *Angew. Chem. Int. Ed.* **2008**, *47*, 8280.
[5] O. Grassmann, P. Lobmann, *Biomaterials* **2004**, *25*, 277.
[6] G. Falini, *Int. J. Inorg. Mater.* **2000**, *2*, 455.
[7] F. C. Meldrum, H. Cölfen, *Chem. Rev.* **2008**, *108*, 4332.
[8] L. Silverman, A. L. Boskey, *Calcif. Tissue Int.* **2004**, *75*, 494.
[9] Y. Shi, J. Q. Geng, D. Yang, *Prog. Chem.* **2010**, *22*, 2224.
[10] Y. Levi-Kalisman, G. Falini, L. Addadi, S. Weiner, *J. Struct. Biol.* **2001**, *135*, 8.
[11] L. Addadi, D. Joester, F. Nudelman, S. Weiner, *Chem. Eur. J.* **2006**, *12*, 981.
[12] J. S. Evans, *Chem. Rev.* **2008**, *108*, 4455.
[13] P. L. Clode, A. T. Marshall, *Protoplasma* **2003**, *220*, 153.
[14] B. Constantz, S. Weiner, *J. Exp. Zool.* **1988**, *248*, 253.
[15] Y. Dauphin, *Int. J. Biol. Macromol.* **2001**, *28*, 293.
[16] I. Sondi, B. Salopek-Sondi, S. D. Skapin, S. Segota, I. Jurina, B. Vukelic, *J. Colloid Interface Sci.* **2011**, *354*, 181.
[17] H. Ehrlich, P. Etnoyer, S. D. Litvinov, M. M. Olennikova, H. Domaschke, T. Hanke, R. Born, H. Meissner, H. Worch, *Materialwiss. Werkst.* **2006**, *37*, 552.
[18] S. Tambutté, E. Tambutté, D. Zoccola, D. Allemand, in *Handbook of Biomineralization*, (Ed: E. Bäuerlein), Wiley-VCH Verlag GmbH & Co., Weinheim **2007**.
[19] I. Sethmann, U. Helbig, G. Worheide, *CrystEngComm* **2007**, *9*, 1262.
[20] D. J. Lim, *Ann. Oto. Rhinol. Laryn.* **1983**, *93*, 17.
[21] U. Lins, M. Farina, M. Kurc, G. Riordan, R. Thalmann, I. Thalmann, B. Kachar, *J. Struct. Biol.* **2000**, *131*, 67.
[22] K. G. Pote, M. D. Ross, *Comp. Biochem. Physiol., B: Biochem. Molec. Biol.* **1991**, *98*, 287.
[23] Y. X. Wang, P. E. Kowalski, I. Thalmann, D. M. Ornitz, D. L. Mager, R. Thalmann, *Proc. Natl. Acad. Sci. USA* **1998**, *95*, 15345.
[24] Y. F. Xu, H. Zhang, H. Yang, X. Zhao, S. Lovas, Y. W. Lundberg, *Dev. Dynam.* **2010**, *239*, 2659.
[25] J. G. Davis, J. C. Oberholtzer, F. R. Burns, M. I. Greene, *Science* **1995**, *267*, 1031.
[26] G. Falini, S. Fermani, S. Vanzo, M. Miletic, G. Zaffino, *Eur. J.Inorg. Chem.* **2005**, 162.
[27] R. W. Gauldie, *J. Morphol.* **1993**, *218*, 1.
[28] I. Hughes, L. Blasiole, D. Huss, M. E. Warchol, N. P. Rath, B. Hurle, E. Ignatova, J. D. Dickman, R. Thalmann, R. Levenson, D. M. Ornitz, *Dev. Biol.* **2004**, *276*, 391.
[29] E. Murayama, P. Herbomel, A. Kawakami, H. Takeda, H. Nagasawa, *Mech. Develop.* **2005**, *122*, 791.
[30] E. Murayama, Y. Takagi, T. Ohira, J. G. Davis, M. I. Greene, H. Nagasawa, *Eur. J. Biochem.* **2002**, *269*, 688.
[31] A. M. Oliveira, M. Farina, I. P. Ludka, B. Kachar, *Naturwissenschaften* **1996**, *83*, 133.
[32] Y. Mugiya, *Fish B-NOAA* **1987**, *85*, 395.
[33] E. Murayama, A. Okuno, T. Ohira, Y. Takagi, H. Nagasawa, *Comp. Biochem. Physiol., B: Biochem. Molec. Biol.* **2000**, *126*, 511.
[34] G. M. Khalifa, S. Weiner, L. Addadi, *Cryst. Growth Des.* **2011**, *11*, 5122.

[35] J. Moradian-Oldak, *Matrix Biol.* **2001**, *20*, 293.
[36] M. Iijima, J. Moradian-Oldak, *J. Mater. Chem.* **2004**, *14*, 2189.
[37] H. C. Margolis, E. Beniash, C. E. Fowler, *J. Dent. Res.* **2006**, *85*, 775.
[38] P. A. Fang, J. F. Conway, H. C. Margolis, J. P. Simmer, E. Beniash, *Proc. Natl. Acad. Sci. USA* **2011**, *108*, 14097.
[39] S. Weiner, H. D. Wagner, *Annu. Rev. Mater. Sci.* **1998**, *28*, 271.
[40] H. Lowenstam, S. Weiner, *On Biomineralization*, Oxford University Press, New York **1989**.
[41] A. L. Boskey, *Bone Miner.* **1989**, *6*, 111.
[42] A. George, A. Veis, *Chem. Rev.* **2008**, *108*, 4670.
[43] K. M. Towe, H. A. Lowenstam, *J. Ultrastruct. Res.* **1967**, *17*, 1.
[44] L. M. Gordon, D. Joester, *Nature* **2011**, *469*, 194.
[45] E. D. Sone, S. Weiner, L. Addadi, *J. Struct. Biol.* **2007**, *158*, 428.
[46] S. Weiner, P. M. Dove, in *Biomineralization*, Vol. 54 (Eds: P. M. Dove, J. J. DeYoreo, S. Weiner), The Mineralogical Society of America, Washington, D.C. **2003**.
[47] A. Veis, in *Biomineralization*, Vol. 54 (Eds: P. M. Dove, J. J. DeYoreo, S. Weiner), The Mineralogical Society of America, Washington, D.C. **2003**.
[48] S. Mann, *Biomineralization: Principles and Concepts in Bioinorganic Materials Chemistry*, Oxford University Press, New York **2001**.
[49] S. Weiner, L. Addadi, *J. Mater. Chem.* **1997**, *7*, 689.
[50] S. Weiner, *Am. Zool.* **1984**, *24*, 945.
[51] A. P. Jackson, J. F. V. Vincent, R. M. Turner, *Proc. R. Soc. London, Ser. B* **1988**, *234*, 415.
[52] J. Aizenberg, A. Tkachenko, S. Weiner, L. Addadi, G. Hendler, *Nature* **2001**, *412*, 819.
[53] Y. Ma, S. R. Cohen, L. Addadi, S. Weiner, *Adv. Mater.* **2008**, *20*, 1555.
[54] F. Nudelman, E. Shimoni, E. Klein, M. Rousseau, X. Bourrat, E. Lopez, L. Addadi, S. Weiner, *J. Struct. Biol.* **2008**, *162*, 290.
[55] G. Falini, S. Albeck, S. Weiner, L. Addadi, *Science* **1996**, *271*, 67.
[56] S. Albeck, S. Weiner, L. Addadi, *Chem. Eur. J.* **1996**, *2*, 278.
[57] F. Nudelman, H. H. Chen, H. A. Goldberg, S. Weiner, L. Addadi, *Faraday Discuss.* **2007**, *136*, 9.
[58] H. Y. Li, H. L. Xin, D. A. Muller, L. A. Estroff, *Science* **2009**, *326*, 1244.
[59] H. Imai, T. Terada, S. Yamabi, *Chem. Commun.* **2003**, 484.
[60] O. Grassmann, R. B. Neder, A. Putnis, P. Löbmann, *Am. Mineral.* **2003**, *88*, 647.
[61] Y. Oaki, H. Imai, *Cryst. Growth Des.* **2003**, *3*, 711.
[62] Y. Oaki, S. Hayashi, H. Imai, *Chem. Commun.* **2007**, 2841.
[63] K. Almdal, J. Dyre, S. Hvidt, O. Kramer, *Makromol. Chem., Macromol. Symp.* **1993**, *76*, 49.
[64] G. M. Kavanagh, S. B. Ross-Murphy, *Prog. Polym. Sci.* **1998**, *23*, 533.
[65] P. J. Flory, *Faraday Discuss* **1974**, *57*, 7.
[66] R. Ruchel, R. L. Steere, E. F. Erbe, *J. Chromatogr.* **1978**, *166*, 563.
[67] S. Waki, J. D. Harvey, A. R. Bellamy, *Biopolymers* **1982**, *21*, 1909.
[68] P. Favard, J. P. Lechaire, M. Maillard, N. Favard, M. Djabourov, J. Leblond, *Biol. Cell* **1989**, *67*, 201.
[69] H. H. Trieu, S. Qutubuddin, *Colloid Polym. Sci.* **1994**, *272*, 301.
[70] Z. Blank, A. C. Reimschuessel, *J. Mater. Sci.* **1974**, *9*, 1815.
[71] N. Pernodet, M. Maaloum, B. Tinland, *Electrophoresis* **1997**, *18*, 55.
[72] E. S. Halberstadt, H. K. Henisch, J. Nickl, E. W. White, *J. Colloid Interface Sci.* **1969**, *29*, 469.
[73] C. Geiger, M. Stanescu, L. H. Chen, D. G. Whitten, *Langmuir* **1999**, *15*, 2241.
[74] L. A. Estroff, A. D. Hamilton, *Chem. Rev.* **2004**, *104*, 1201.
[75] K. Y. Lee, D. J. Mooney, *Chem. Rev.* **2001**, *101*, 1869.
[76] S. Van Vlierberghe, P. Dubruel, E. Schacht, *Biomacromolecules* **2011**, *12*, 1387.
[77] A. Veis, *The Macromolecular Chemistry of Gelatin*, Academic Press, New York **1964**.
[78] R. G. Weiss, P. Terech, *Molecular Gels: Materials with Self-Assembled Fibrillar Networks*, Springer, Netherlands **2006**.
[79] E. Tsuchida, K. Abe, *Adv. Polym. Sci.* **1982**, *45*, 1.
[80] M. Rinaudo, *Polym. Int.* **2008**, *57*, 397.
[81] M. Lahaye, C. Rochas, *Hydrobiologia* **1991**, *221*, 137.
[82] S. Arnott, A. Fulmer, W. E. Scott, I. C. M. Dea, R. Moorhouse, D. A. Rees, *J. Mol. Biol.* **1974**, *90*, 269.
[83] J. M. Guenet, C. Rochas, *Macromol. Symp.* **2006**, *242*, 65.
[84] K. B. Guiseley, (Union, ME), US Patent 3956273, **1976**.
[85] V. Normand, D. L. Lootens, E. Amici, K. P. Plucknett, P. Aymard, *Biomacromolecules* **2000**, *1*, 730.
[86] J. F. Zhou, M. F. Zhou, R. A. Caruso, *Langmuir* **2006**, *22*, 3332.
[87] M. Maaloum, N. Pernodet, B. Tinland, *Electrophoresis* **1998**, *19*, 1606.
[88] S. Whytock, J. Finch, *Biopolymers* **1991**, *31*, 1025.
[89] G. A. Griess, K. B. Guiseley, P. Serwer, *Biophys. J.* **1993**, *65*, 138.
[90] U.-J. Kim, J. Park, C. Li, H.-J. Jin, R. Valluzzi, D. L. Kaplan, *Biomacromolecules* **2004**, *5*, 786.
[91] C. Vepari, D. L. Kaplan, *Prog. Polym. Sci.* **2007**, *32*, 991.
[92] A. Matsumoto, J. Chen, A. L. Collette, U.-J. Kim, G. H. Altman, P. Cebe, D. L. Kaplan, *J. Phys. Chem. B* **2006**, *110*, 21630.
[93] E. C. Keene, *Ph. D. Thesis*. Cornell University, Ithaca, NY **2010**.
[94] J. E. Eastoe, *Biochem. J.* **1955**, *61*, 589.
[95] D. Voet, J. G. Voet, C. W. Pratt, in *Fundamentals of Biochemistry*, John Wiley & Sons, New York **2002**.
[96] A. J. Kuijpers, G. H. M. Engbers, J. Feijen, S. C. De Smedt, T. K. L. Meyvis, J. Demeester, J. Krijgsveld, S. A. J. Zaat, J. Dankert, *Macromolecules* **1999**, *32*, 3325.
[97] H. J. Naghash, O. Okay, *J. Appl. Polym. Sci.* **1996**, *60*, 971.
[98] A. Suzuki, M. Yamazaki, Y. Kobiki, *J. Chem. Phys.* **1996**, *104*, 1751.
[99] U. Helbig, *J. Cryst. Growth* **2008**, *310*, 2863.
[100] T. P. Hsu, C. Cohen, *Polymer* **1984**, *25*, 1419.
[101] R. K. Iler, *The Chemistry of Silica: Solubility, Polymerization, Colloid and Surface Properties, and Biochemistry*, John Wiley & Sons, New York **1979**.
[102] C. J. Plank, *J. Colloid Sci.* **1947**, *2*, 413.
[103] C. B. Hurd, *J. Phys. Chem.* **1936**, *40*, 21.
[104] R. C. Merrill, R. W. Spencer, *J. Phys. Colloid Chem.* **1950**, *54*, 806.
[105] O. Vidal, M. C. Robert, F. Boue, *J. Cryst. Growth* **1998**, *192*, 271.
[106] E. G. Acker, *J. Colloid Interface Sci.* **1970**, *32*, 41.
[107] W. Drost-Hansen, *Ind. Eng. Chem.* **1969**, *61*, 10.
[108] R. J. Mashl, S. Joseph, N. R. Aluru, E. Jakobsson, *Nano Lett.* **2003**, *3*, 589.
[109] B. Ratajska-Gadomska, B. Bialkowski, W. Gadomski, C. Radzewicz, *J. Chem. Phys.* **2007**, *126*, 184708.
[110] Y. Sekine, T. Ikeda-Fukazawa, *J. Chem. Phys.* **2009**, *130*.
[111] T. Singh, R. Meena, A. Kumar, *J. Phys. Chem. B* **2009**, *113*, 2519.
[112] B. Ratajska-Gadomska, W. Gadomski, *J. Chem. Phys.* **2004**, *121*, 12583.
[113] T. Goda, J. Watanabe, M. Takai, K. Ishihara, *Polymer* **2006**, *47*, 1390.
[114] F. V. Chavez, E. Persson, B. Halle, *J. Am. Chem. Soc.* **2006**, *128*, 4902.
[115] M. S. Jhon, J. D. Andrade, *J. Biomed. Mater. Res.* **1973**, *7*, 509.
[116] H. B. Lee, M. S. Jhon, J. D. Andrade, *J. Colloid Interface Sci.* **1975**, *51*, 225.
[117] M. Aizawa, S. Suzuki, *Bull. Chem. Soc. Jpn.* **1971**, *44*, 2967.
[118] J. Garside, R. Davey, *From Molecules to Crystallizers: An Introduction to Crystallization*, Oxford University Press, New York **2000**.
[119] A. A. Chernov, *Modern Crystallography III: Crystal Growth*, Vol. *36* Springer-Verlag, New York **1984**.

[120] J. J. De Yoreo, P. Vekilov, in *Reviews in Mineralogy and Geochemistry: Biomineralization*, Vol. *54* (Eds: P. M. Dove, J. J. D. Yoreo, S. Weiner), The Mineralogical Society of America, Washington, D. C. **2003**.
[121] I. Sunagawa, *Growth, Morphology and Perfection*, Cambridge University Press, Cambridge **2005**.
[122] I. Sunagawa, *B. Mineral.* **1981**, *104*, 81.
[123] J. M. Garcia-Ruiz, J. A. Gavira, F. Otalora, A. Guasch, M. Coll, *Mater. Res. Bull.* **1998**, *33*, 1593.
[124] F. Sica, D. Demasi, L. Mazzarella, A. Zagari, S. Capasso, L. H. Pearl, S. Dauria, C. A. Raia, M. Rossi, *Acta Crystallogr. Sect. D-Biol. Crystallogr.* **1994**, *50*, 508.
[125] O. Vidal, M. C. Robert, B. Arnoux, B. Capelle, *J. Cryst. Growth* **1999**, *196*, 559.
[126] B. Lorber, C. Sauter, J. D. Ng, D. W. Zhu, R. Giege, O. Vidal, M. C. Robert, B. Capelle, *J. Cryst. Growth* **1999**, *204*, 357.
[127] T. Y. Miller, X.-M. He, D. C. Carter, *J. Cryst. Growth* **1992**, *122*, 306.
[128] B. Lorber, C. Sauter, A. Theobald-Dietrich, A. Moreno, P. Schellenberger, M. C. Robert, B. Capelle, S. Sanglier, N. Potier, R. Giege, *Prog. Biophys. Mol. Biol.* **2009**, *101*, 13.
[129] Z. Pietras, H. T. Lin, S. Surade, B. Luisi, O. Slattery, K. M. Pos, A. Moreno, *J. Appl. Crystallogr.* **2010**, *43*, 58.
[130] M. Prieto, A. Putnis, L. Fernández-Díaz, S. Lûpez-Andrès, *J. Cryst. Growth* **1994**, *142*, 225.
[131] D. Srzic, B. Pokric, Z. Pucar, *Z. Phys. Chem.* **1976**, *103*, 157.
[132] Z. Pučar, B. Pokrić, A. Graovac, *Anal. Chem.* **1974**, *46*, 403.
[133] A. Putnis, M. Prieto, L. Fernández-Díaz, *Geol. Mag.* **1995**, *132*, 1.
[134] P. Andreazza, F. Lefaucheux, B. Mutaftschiev, *J. Cryst. Growth* **1988**, *92*, 415.
[135] J. Dennis, H. K. Henisch, *J. Electrochem. Soc.* **1967**, *114*, 263.
[136] K. Provost, M. C. Robert, *J. Cryst. Growth* **1991**, *110*, 258.
[137] A. E. S. Van Driessche, F. Otalora, J. A. Gavira, G. Sazaki, *Cryst. Growth Des.* **2008**, *8*, 3623.
[138] K. Tanabe, M. Hirose, R. Murai, S. Sugiyama, N. Shimizu, M. Maruyama, Y. Takahashi, H. Adachi, K. Takano, S. Murakami, Y. Mori, E. Mizohata, T. Inoue, H. Matsumura, *Appl. Phys. Express* **2009**, *2*.
[139] H. Imai, Y. Oaki, *CrystEngComm* **2010**, *12*, 1679.
[140] J. M. Garcìa-Ruìz, *J. Cryst. Growth* **1986**, *75*, 441.
[141] *CRC Handbook of Chemistry and Physics*, (Ed: D. R. Lide), CRC Press, Boca Raton, FL **2007**.
[142] R. I. Petrova, J. A. Swift, *J. Am. Chem. Soc.* **2004**, *126*, 1168.
[143] R. I. Petrova, R. Patel, J. A. Swift, *Cryst. Growth Des.* **2006**, *6*, 2709.
[144] R. I. Petrova, J. A. Swift, *Cryst. Growth Des.* **2002**, *2*, 573.
[145] O. Grassmann, G. Muller, P. Lobmann, *Chem. Mater.* **2002**, *14*, 4530.
[146] L. A. Estroff, L. Addadi, S. Weiner, A. D. Hamilton, *Org. Biomol. Chem.* **2004**, *2*, 137.
[147] H. J. Nickl, H. K. Henisch, *J. Electrochem. Soc.* **1969**, *116*, 1258.
[148] J. A. Gavira, J. M. García-Ruiz, *Acta Crystallogr. Sect. D-Biol. Crystallogr.* **2002**, *58*, 1653.
[149] H. Li, Y. Fujiki, K. Sada, L. A. Estroff, *CrystEngComm* **2011**, *13*, 1060.
[150] A. Patel, A. Venkateswara Rao, *Bull. Mater. Sci.* **1982**, *4*, 527.
[151] M. Prieto, L. Fernández-Díaz, L. Lûpez-Andrès, S. Lûpez-Andrès, *J. Cryst. Growth* **1989**, *98*, 447.
[152] J. R. Dorvee, A. L. Boskey, L. A. Estroff, *CrystEngComm* **2012**, accepted DOI: 10.1039/C2CE25289A.
[153] C. M. Pina, L. Fernández-Díaz, M. Prieto, *J. Cryst. Growth* **1997**, *177*, 102.
[154] B. A. Gotliv, L. Addadi, S. Weiner, *ChemBioChem* **2003**, *4*, 522.
[155] F. Nudelman, B. A. Gotliv, L. Addadi, S. Weiner, *J. Struct. Biol.* **2006**, *153*, 176.
[156] S. Sudo, T. Fujikawa, T. Nagakura, T. Ohkubo, K. Sakaguchi, M. Tanaka, K. Nakashima, T. Takahashi, *Nature* **1997**, *387*, 563.
[157] S. Weiner, W. Traub, *FEBS Lett.* **1980**, *111*, 311.
[158] S. Weiner, Y. Talmon, W. Traub, *Int. J. Biol. Macromol.* **1983**, *5*, 325.
[159] H. Ehrlich, P. G. Koutsoukos, K. D. Demadis, O. S. Pokrovsky, *Micron* **2009**, *40*, 169.
[160] R. Przenioslo, J. Stolarski, M. Mazur, M. Brunelli, *J. Struct. Biol.* **2008**, *161*, 74.
[161] S. A. Wainwright, *Exp. Cell Res.* **1964**, *34*, 213.
[162] R. J. Kingsley, M. Tsuzaki, N. Watabe, G. L. Mechanic, *Biol. Bull.* **1990**, *179*, 207.
[163] E. A. Rosauer, J. R. Redmond, *J. Laryngol. Otol.* **1985**, *99*, 21.
[164] P. Simon, W. Carrillo-Cabrera, Y. X. Huang, J. Buder, H. Borrmann, R. Cardoso-Gil, E. Rosseeva, Y. Yarin, T. Zahnert, R. Kniep, *Eur. J. Inorg. Chem.* **2011**, 5370.
[165] C. D. Fermin, *Microsc. Res. Tech.* **1993**, *25*, 297.
[166] X. Zhao, H. Yang, E. N. Yamoah, Y. W. Lundberg, *Dev. Biol.* **2007**, *304*, 508.
[167] J. G. Davis, F. R. Burns, D. Navaratnam, A. M. Lee, S. Ichimiya, J. C. Oberholtzer, M. I. Greene, *Proc. Natl. Acad. Sci. USA* **1997**, *94*, 707.
[168] G. Falini, S. Fermani, M. Gazzano, A. Ripamonti, *Chem. Eur. J.* **1997**, *3*, 1807.
[169] E. C. Keene, J. S. Evans, L. A. Estroff, *Cryst. Growth Des.* **2010**, *10*, 5169.
[170] A. Mata, Y. B. Geng, K. J. Henrikson, C. Aparicio, S. R. Stock, R. L. Satcher, S. I. Stupp, *Biomaterials* **2010**, *31*, 6004.
[171] S. Busch, U. Schwarz, R. Kniep, *Chem. Mater.* **2001**, *13*, 3260.
[172] K. Gkioni, S. C. G. Leeuwenburgh, T. E. L. Douglas, A. G. Mikos, J. A. Jansen, *Tissue Eng. Part B-Rev.* **2010**, *16*, 577.
[173] H. Y. Li, L. A. Estroff, *CrystEngComm* **2007**, *9*, 1153.
[174] L. Pastero, E. Costa, B. Alessandria, M. Rubbo, D. Aquilano, *J. Cryst. Growth* **2003**, *247*, 472.
[175] D. Yang, L. M. Qi, J. M. Ma, *Chem. Commun.* **2003**, 1180.
[176] J. Watanabe, M. Akashi, *Cryst. Growth Des.* **2008**, *8*, 478.
[177] B. M. Borah, H. Lakshmi, G. Das, *Mater. Sci. Eng. C* **2008**, *28*, 1173.
[178] N. Wada, K. Yamashita, T. Umegaki, *J. Cryst. Growth* **1995**, *148*, 297.
[179] N. Wada, K. Yamashita, T. Umegaki, *J. Colloid Interface Sci.* **1998**, *201*, 1.
[180] N. Wada, M. Okazaki, S. Tachikawa, *J. Cryst. Growth* **1993**, *132*, 115.
[181] N. Wada, K. Yamashita, T. Umegaki, *J. Colloid Interface Sci.* **1999**, *212*, 357.
[182] S. Boggavarapu, J. Chang, P. Calvert, *Mater. Sci. Eng. C* **2000**, *11*, 47.
[183] K. Kayano, K. Saruwatari, T. Kogure, Y. Shiraiwa, *Marine Biotechnol.* **2011**, *13*, 83.
[184] M. F. Butler, N. Glaser, A. C. Weaver, M. Kirkland, M. Heppenstall-Butler, *Cryst. Growth Des.* **2006**, *6*, 781.
[185] C. Kosanovi , G. Falini, D. Kralj, *Cryst. Growth Des.* **2011**, *11*, 269.
[186] Y. Ma, Q. Feng, *J. Solid State Chem.* **2011**, *184*, 1008.
[187] M. Xie, M. O. Olderøy, J.-P. Andreassen, S. M. Selbach, B. L. Strand, P. Sikorski, *Acta Biomater.* **2010**, *6*, 3665.
[188] M. O. Olderøy, M. L. Xie, B. L. Strand, E. M. Flaten, P. Sikorski, J. P. Andreassen, *Cryst. Growth Des.* **2009**, *9*, 5176.
[189] J. W. Xiao, Y. C. Zhu, Y. Y. Liu, H. J. Liu, Y. Zeng, F. F. Xu, L. Z. Wang, *Cryst. Growth Des.* **2008**, *8*, 2887.
[190] N. H. Munro, D. W. Green, A. Dangerfield, K. M. McGrath, *Dalton Trans.* **2011**, *40*, 9259.
[191] M. L. Xie, M. O. Olderøy, J. P. Andreassen, S. M. Selbach, B. L. Strand, P. Sikorski, *Acta Biomater.* **2010**, *6*, 3665.
[192] X. P. Li, Q. Shen, Y. L. Su, F. Tian, Y. Zhao, D. J. Wang, *Cryst. Growth Des.* **2009**, *9*, 3470.
[193] N. H. Munro, K. M. McGrath, *Dalton Trans.* **2011**, *40*, 9269.
[194] G. Falini, S. Fermani, M. Gazzano, A. Ripamonti, *Chem. Eur. J.* **1998**, *4*, 1048.

[195] G. Falini, S. Fermani, M. Gazzano, A. Ripamonti, *J. Chem. Soc., Dalton Trans.* **2000**, 3983.
[196] G. Falini, M. Gazzano, A. Ripamonti, *Adv. Mater.* **1994**, *6*, 46.
[197] J. W. Xiao, S. H. Yang, *CrystEngComm* **2011**, *13*, 2472.
[198] G. Falini, M. Gazzano, A. Ripamonti, *J. Cryst. Growth* **1994**, *137*, 577.
[199] O. Grassmann, P. Lobmann, *Chem. Eur. J.* **2003**, *9*, 1310.
[200] J. W. McCauley, R. Roy, *Am. Mineral.* **1974**, *59*, 947.
[201] S. Dominguez-Bella, J. M. García-Ruiz, *J. Cryst. Growth* **1986**, *79*, 236.
[202] L. Fernández-Díaz, A. Putnis, M. Prieto, C. V. Putnis, *J. Sediment. Res.* **1996**, *66*, 482.
[203] L. Fernández-Díaz, J. M. Astilleros, C. M. Pina, *Chem. Geol.* **2006**, *225*, 314.
[204] H. Imai, T. Terada, T. Miura, S. Yamabi, *J. Cryst. Growth* **2002**, *244*, 200.
[205] J. M. García-Ruiz, *J. Cryst. Growth* **1985**, *73*, 251.
[206] D. Katsikopoulos, A. Fernández-González, M. Prieto, *Mineral. Mag.* **2009**, *73*, 269.
[207] D. Katsikopoulos, A. Fernández-González, A. C. Prieto, M. Prieto, *Chem. Geol.* **2008**, *254*, 87.
[208] C. Barta, J. Zemlicka, V. Rene, *J. Cryst. Growth* **1971**, *10*, 158.
[209] M. Prieto, J. M. García-Ruiz, J. L. Amoros, *J. Cryst. Growth* **1981**, *52*, 864.
[210] N. Sánchez-Pastor, A. M. Gigler, J. A. Cruz, S.-H. Park, G. Jordan, L. Fernández-Díaz, *Cryst. Growth Des.* **2011**, *11*, 3081.
[211] M. Prieto, A. Fernández-González, A. Putnis, L. Fernández-Díaz, *Geochim. Cosmochim. Acta* **1997**, *61*, 3383.
[212] E. C. Keene, J. S. Evans, L. A. Estroff, *Cryst. Growth Des.* **2010**, *10*, 1383.
[213] M. Kuang, D. Y. Wang, M. Y. Gao, J. Hartmarm, H. Mohwald, *Chem. Mater.* **2005**, *17*, 656.
[214] N. Shi, G. Yin, M. Han, Z. Xu, *Colloid Surf. B* **2008**, *66*, 84.
[215] A. M. Belcher, X. H. Wu, R. J. Christensen, P. K. Hansma, G. D. Stucky, D. E. Morse, *Nature* **1996**, *381*, 56.
[216] Y. Levi, S. Albeck, A. Brack, S. Weiner, L. Addadi, *Chem. Eur. J.* **1998**, *4*, 389.
[217] G. Falini, G. Sartor, D. Fabbri, P. Vergni, S. Fermani, A. M. Belcher, G. D. Stucky, D. E. Morse, *J. Struct. Biol.* **2011**, *173*, 128.
[218] G. Falini, S. Weiner, L. Addadi, *Calcif. Tissue Int.* **2003**, *72*, 548.
[219] C. Cheng, Z. Z. Shao, F. Vollrath, *Adv. Funct. Mater.* **2008**, *18*, 2172.
[220] X. Q. An, C. B. Cao, *J. Phys. Chem. C* **2008**, *112*, 15844.
[221] X. Q. An, C. B. Cao, *J. Phys. Chem. C* **2008**, *112*, 6526.
[222] T. Wang, R. C. Che, W. T. Li, R. X. Mi, Z. Z. Shao, *Cryst. Growth Des.* **2011**, *11*, 2164.
[223] Y. D. Wu, C. Cheng, J. R. Yao, X. Chen, Z. Z. Shao, *Langmuir* **2011**, *27*, 2804.
[224] H. Imai, Y. Oaki, A. Kotachi, *Bull. Chem. Soc. Jpn.* **2006**, *79*, 1834.
[225] S. Raz, S. Weiner, L. Addadi, *Adv. Mater.* **2000**, *12*, 38.
[226] S. Mann, J. M. Didymus, N. P. Sanderson, B. R. Heywood, E. J. A. Samper, *J. Chem. Soc., Faraday Trans.* **1990**, *86*, 1873.
[227] Y. J. Han, J. Aizenberg, *J. Am. Chem. Soc.* **2003**, *125*, 4032.
[228] B. Cantaert, Y.-Y. Kim, H. Ludwig, F. Nudelman, N. A. J. M. Sommerdijk, F. C. Meldrum, *Adv. Funct. Mater.* **2012**, *22*, 907.
[229] K. Gries, R. Kroger, C. Kubel, M. Fritz, A. Rosenauer, *Acta Biomater.* **2009**, *5*, 3038.
[230] J. S. Robach, S. R. Stock, A. Veis, *J. Struct. Biol.* **2005**, *151*, 18.
[231] J. Aizenberg, J. Hanson, T. F. Koetzle, S. Weiner, L. Addadi, *J. Am. Chem. Soc.* **1997**, *119*, 881.
[232] A. Berman, J. Hanson, L. Leiserowitz, T. F. Koetzle, S. Weiner, L. Addadi, *Science* **1993**, *259*, 776.
[233] J. Aizenberg, D. A. Muller, J. L. Grazul, D. R. Hamann, *Science* **2003**, *299*, 1205.
[234] A. S. Finnemore, M. R. J. Scherer, R. Langford, S. Mahajan, S. Ludwigs, F. C. Meldrum, U. Steiner, *Adv. Mater.* **2009**, *21*, 3928.
[235] C. Li, L. M. Qi, *Angew. Chem. Int. Ed.* **2008**, *47*, 2388.
[236] R. J. Park, F. C. Meldrum, *J. Mater. Chem.* **2004**, *14*, 2291.
[237] N. B. J. Hetherington, A. N. Kulak, K. Sheard, F. C. Meldrum, *Langmuir* **2006**, *22*, 1955.
[238] R. Muñoz-Espí, A. Chandra, G. Wegner, *Cryst. Growth Des.* **2007**, *7*, 1584.
[239] C. H. Lu, L. M. Qi, H. L. Cong, X. Y. Wang, J. H. Yang, L. L. Yang, D. Y. Zhang, J. M. Ma, W. X. Cao, *Chem. Mater.* **2005**, *17*, 5218.
[240] Y. Y. Kim, L. Ribeiro, F. Maillot, O. Ward, S. J. Eichhorn, F. C. Meldrum, *Adv. Mater.* **2010**, *22*, 2082.
[241] Y. X. Huang, J. Burder, R. Cardoso-Gli, Y. Prots, W. Carrillo-Cabrera, P. Simon, R. Kniep, *Angew. Chem. Int. Ed.* **2008**, *47*, 8280.
[242] M. G. Page, N. Nassif, H. G. Borner, M. Antonietti, H. Colfen, *Cryst. Growth Des.* **2008**, *8*, 1792.
[243] Y. Y. Kim, K. Ganesan, P. C. Yang, A. N. Kulak, S. Borukhin, S. Pechook, L. Ribeiro, R. Kroger, S. J. Eichhorn, S. P. Armes, B. Pokroy, F. C. Meldrum, *Nat. Mater.* **2011**, *10*, 890.
[244] H. Y. Li, L. A. Estroff, *J. Am. Chem. Soc.* **2007**, *129*, 5480.
[245] V. I. Khaimov-Mal'kov, *Sov. Phys.: Crystallogr.* **1958**, *3*, 487.
[246] J. I. Hanoka, *J. Appl. Phys.* **1969**, *40*, 2694.
[247] F. Lefaucheux, M. C. Robert, Y. Bernard, S. Gits, *Cryst. Res. Technol.* **1984**, *19*, 1541.
[248] A. A. Chernov, D. E. Temkin, in *Current Topics in Materials Science*, Vol. *2* (Ed: E. Kaldis), North-Holland, New York **1977**.
[249] M. O. Kliya, I. G. Sokolova, *Sov. Phys. Crystallogr.* **1958**, *3*, 217.
[250] D. R. Uhlmann, B. Chalmers, K. A. Jackson, *J. Appl. Phys.* **1964**, *35*, 2986.
[251] J. Aizenberg, A. J. Black, G. M. Whitesides, *Nature* **1999**, *398*, 495.
[252] A. A. Chernov, D. E. Temkin, A. M. Melnikova, *Kristallografiya* **1976**, *21*, 652.
[253] F. C. Meldrum, *Int. Mater. Rev.* **2003**, *48*, 187.
[254] N. Sommerdijk, G. de With, *Chem. Rev.* **2008**, *108*, 4499.